Formation Control of the Purcell's swimmer

Master's Thesis
Submitted in partial fulfillment of
the requirements for the degree of
Master of Technology
by

Pulkit Katdare
(130100006)

Department of Mechanical Engineering
Indian Institute of Technology Bombay
Mumbai 400076 (India)

5 September 2023

Dedicated to My Mother, Kalyani Katdare and Father, Milind Katdare

Abstract

Co-ordination control is the synthesized movment of two or more autonomous entities to achieve a desired goal. In this Thesis, we present a formation control problem in the context of the Purcell's swimmer, the primitive micro-swimmer capable of generating locomotion at a micro-scopic scale. As it is with all co-ordination problems, first task in this report has been to investigate the communication protocol between these two micro-robotic swimmers. Using this and only this protocol we first present co-ordination problem wherein the two-swimmers start executing a circular trajectory around each other. Not only a control formulation we also prove the asymptotic stability of this circular formation problem by using Lyapunov's Theorem. In the next body of work we extend this circular formulation to achieve a Leader-Follower type of formation in a two-body swimmer wherein the Leader is following an unknown trajectory subject to a bounded velocity. The follower is shown knowing this velocity bound tries to track this Leader using our control formulation. We also extend these control algorithms for state constrained problems to keep our side angles within the desired range of values using a simple transformation.

Table of Contents

List of Figures

List of Tables

Chapter 1

Introduction

There has recently been a strong impetus from the engineering community to study organisms and mechanisms that are able to swim in a microscopic scale in a fluid. The reason behind this is simple, a study at this microscopic scale would enable us engineers to emulate these microscopic designs for robotic applications. These robotic applications not only span medicinal health care but would also turn out to be useful in critical defence missions.

An introductory frame-work to understand these microscopic organisms was first ex-

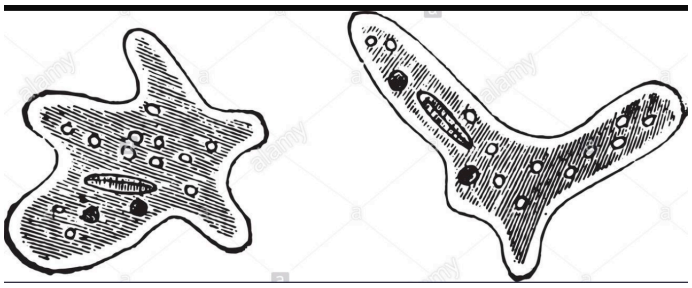

Figure 1.1: Image of an amoeboid

plained by the Nobel Laureate Physicist E.M Purcell in his popular lecture, " life at low Reynolds number "[12]. In this lecture Dr. Purcell laid down important laws that govern a micro-organisms motion in a fluid medium.

According to Purcell due to the sheer small size of these microscopic organisms, the Reynolds number of these microscopic swimming bodies is very small. By definition we say that Reynolds number measures the ratio of the inertial forces to the viscous forces that are being exerted on the microscopic body due to the fluid medium. Hence, a small Reynolds number, ($Re \ll 1$) implies that the net inertial force on the microscopic swimmers almost zero. Not only this, Purcell even went a step further and said that even the net external torque on these swimmers turns out to be zero too.

This simple but important approximation proposed by Purcell not only helps us to get a qualitative understanding of micro-swimmers but also does help in approximating the Navier-Stokes, thus rendering it solvable to help model low Reynolds number motion.

$$\begin{aligned} &\nabla u = 0 \\ &\eta\nabla^2 u = \nabla p + \rho\cancelto{0}{\frac{\partial u}{\partial t}} + \cancelto{0}{\rho(u.\nabla)u} \Rightarrow \eta\nabla^2 u = \nabla p \end{aligned} \tag{1.1}$$

An important consequence of the low Reynolds number approximation is the Scallop theorem, which states that a sequence of configuration changes in the swimmer followed by the exact same sequence in reverse would reverse in a zero net displacement. An example for the scallop theorem can be seen in the figure 1.2 below where a small periodic flap results in a net zero displacement. From the perspective of of control theorists, Scallop theorem is simply a drift-less control affine systems from a modelling perspective which hugely helps in verifying the control models of these swimmers. In accordance with the

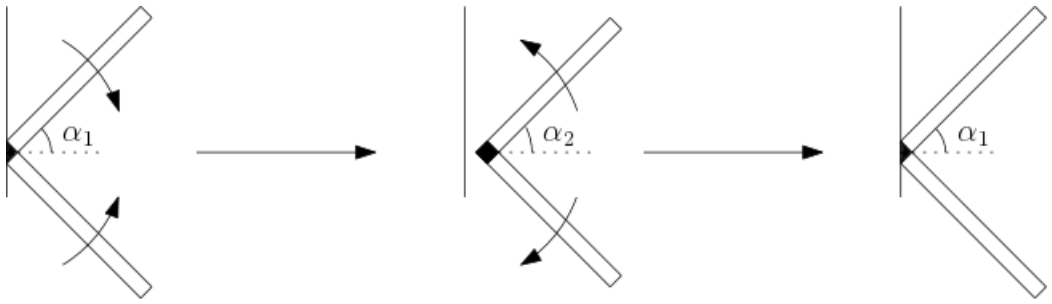

Figure 1.2: Scallop Theorem($\alpha_1 > \alpha_2$)

Scallop theorem, the simplest design which is able to generate motion in a 2D infinite newtonian fluid is the Purcell's swimmer as shown in the figure 1.3. To escape the limitations of the scallop theorem, Purcell's swimmer has three independent but identical slender links. The angle connecting the middle link to the first link from the left is α_1 and similarly the angle connecting the middle link the tertiary one is labelled as α_2.
From control theory perspective, we define the set of controls as the ability to change the angles, α_1 and α_2 by appropriate change in its angular velocity, i.e $u_1 = \dot{\alpha}_1, u_2 = \dot{\alpha}_2$.
To model this, we will need to first determine the lateral and longitudinal force on a slender rod moving in a Newtonian fluid [3] and then using the low Reynolds number approximation that we discussed earlier we can come up with the control model of the

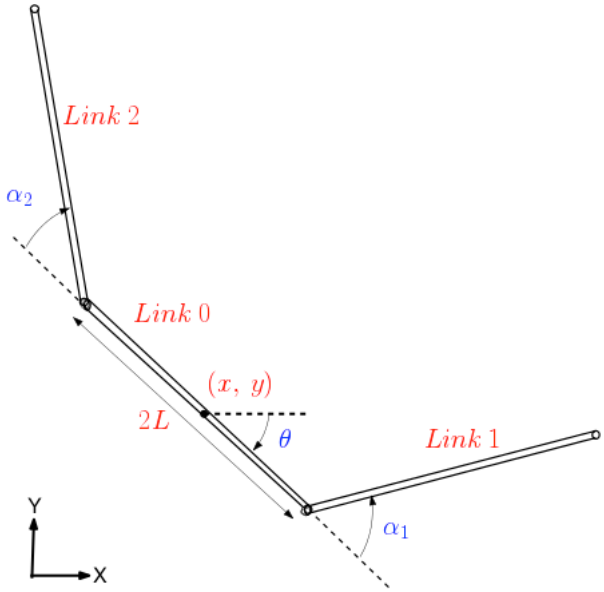

Figure 1.3: Schematic of the Purcell swimmer

Purcell's swimmer [7] as follows,

$$\begin{bmatrix} \dot{x} \\ \dot{y} \\ \dot{\theta} \\ \dot{\alpha}_1 \\ \dot{\alpha}_2 \end{bmatrix} = \begin{bmatrix} A(\alpha_1, \alpha_2) \\ \mathrm{I}_2 \end{bmatrix} \begin{bmatrix} u_1 \\ u_2 \end{bmatrix} \tag{1.2}$$

where, $\dot{x}$ is the direction along the middle link and the $\dot{y}$ is the direction along the direction perpendicular to the middle link. $\dot{\theta}$ is the rate of change in angle of the middle link with respect to an inertial X-axis as shown in the figure. It is important to note here that, $A(\alpha_1, \alpha_2)$ is the map which transforms the swimmers kinematics from the control space to the velocity. This is often regarded as the affine connection form in the differential geometric control literature.

In this report we are going to discuss a control formulation to co-ordinate two or more Purcell swimmers to achieve different formations.

Microscopic robotic swimmers are envision to undertake many potential future applications in healthcare, defence, manufacturing sector. In almost all of these sectors we may need to deploy these micro-robots in synchronization to efficiently realize its applications. This is motivation behind engineering a formation control problem.

It is important to note here that the research to actually fabricate these micro-swimmers is still at a primitive stage with a acute shortage of actuators working at this scale. So this report is entirely a theoretical study with the communication protocol being adopted from formation control literture and moving forward.

In the next chapter we start reviewing the relevant literature in formation control which talks about different control strategies and heuristics that are employed in a formation control problem. In particular we review two important papers that we think cover all the important aspects of formation control theory.

Chapter 2

Literature Survey

There are four major approaches to formation control with respect to the algorithm proposed to implement them, behavorial([11]), virtual structure([1]), Artificial potential trenches([5]) and leader-follower type of formations([8]).
Behavioural based approaches specify the type of behaviours that the formation should follow over and a above maintaining it's own formation. Virtual structure attributes a pre-defined virtual trajectory that each of the agent in the formation should follow, the controllers are designed in order to achieve this particular trajectory and hence the corresponding formation. In queues and potential trench approach, each of the two robot formation is represented as a queue and a particular formation is achieved using artificial potential trench to achieve that formation. In the leader-formation approach, the leader tracks a pre-defined path and the formation tries to achieve a particular geometric configuration with respect to it.
In the section 2.1, we talk about one such leader formation problem for an Unmanned Aerial Vehicle(UAVs). In section 2.2 we again talk about the formation problem for a formation of Autonomous Underwater Vehicle(AUV) using virtual structure approach.

2.1 Leader-Follower Approach

UAV(Unmanned Aerial Vehicle) are a miniature versions of an aircraft which are operated remotely. These vehicles have found applications in earthquake surveillance, border surveying among other things. Many of these applications would require a syncronised co-ordination between swarms of these UAVs for an efficent performance. This article [8] tries to model a planar formation problem for a team of two such UAVs.
We use the Frennet-Serret equations to model these UAVs. In Frennet-Serret equations the UAV is assumed to be moving with a unit velocity($\bar{x}$) and the control effort(u, v, w) is

spent in changing this direction of motion of the UAV.

$$\begin{aligned} \dot{\bar{r}} &= \bar{x} \\ \dot{\bar{x}} &= \bar{y}u - \bar{z}v \\ \dot{\bar{y}} &= -\bar{x}u - \bar{y}w \\ \dot{\bar{z}} &= \bar{x}v - \bar{y}w \end{aligned} \tag{2.1}$$

Here, $\bar{y}, \bar{z}$ are the normal and co-normal vectors of UAVs motion as shown in the figure 2.1

For a planar form of these equations we just put $v, w = 0$. This is illustrated in figure 2.2

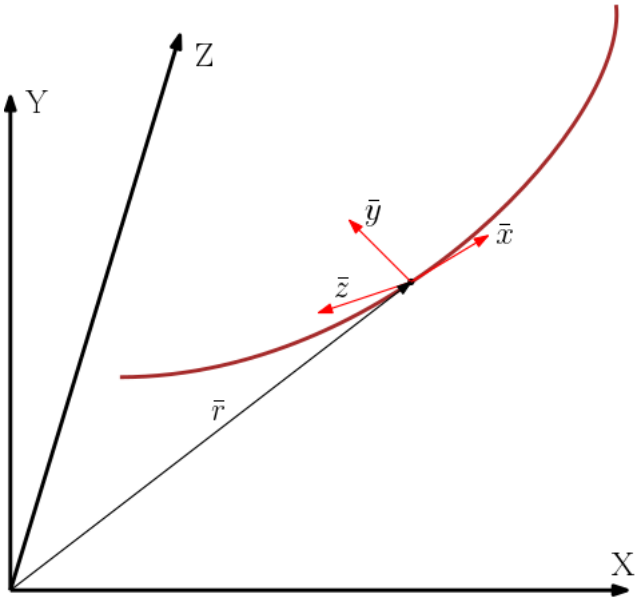

Figure 2.1: Control law terms explained

$$\begin{aligned} \dot{\bar{r}} &= \bar{x} \\ \dot{\bar{x}} &= \bar{y}u \\ \dot{\bar{y}} &= -\bar{x}u \end{aligned} \tag{2.2}$$

2.1.1 Two body planar formation

As shown in the figure 2.2 is a two agent UAV system, where each of them are represented as a point mass. The dynamics of each of these UAVs can be described these equations 2.3 below.

$$\begin{aligned} \dot{\bar{r}}_1 &= \bar{x}_1 & \dot{\bar{r}}_2 &= \bar{x}_2 \\ \dot{\bar{x}}_1 &= \bar{y}_1 u_1 & \dot{\bar{x}}_2 &= \bar{y}_2 u_2 \\ \dot{\bar{y}}_1 &= -\bar{x}_1 u_1 & \dot{\bar{y}}_2 &= -\bar{x}_2 u_2 \end{aligned} \tag{2.3}$$

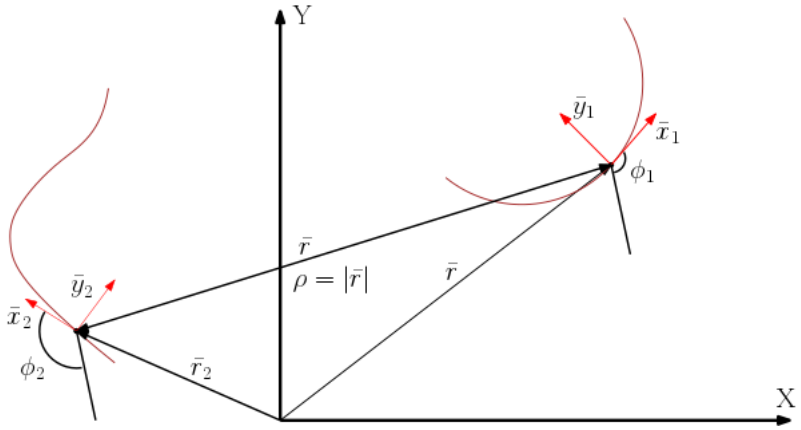

Figure 2.2: planar formation schematic

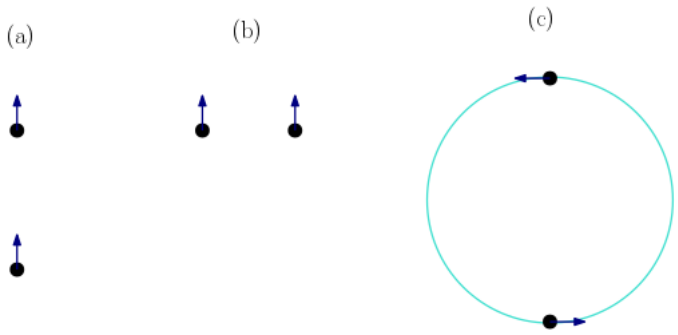

Figure 2.3: Types of UAV formation

Definition 1 (Planar Formation Problem)**.** *Given the initial state of two UAVs, $\bar{r}_1$ and $\bar{r}_2$ respectively. We wish to formulate a control strategy u_1 and u_2 such that this team of two UAVs achieves either one of the formation as described by figure 2.3*

The authors propose the following control law for the system of two UAVs as follows with their dynamics as described in equation 2.2.

$$\begin{aligned} u_1 &= -\eta(|\bar{r}|)(-\frac{\bar{r}}{|\bar{r}|}\cdot\bar{x}_1)(-\frac{\bar{r}}{|\bar{r}|}\cdot\bar{y}_1) - f(|\bar{r}|)(\frac{\bar{r}}{|\bar{r}|}\cdot\bar{y}_1) + \mu(|\bar{r}|)\bar{x}_2\cdot\bar{y}_1 \\ u_2 &= -\eta(|\bar{r}|)(-\frac{\bar{r}}{|\bar{r}|}\cdot\bar{x}_2)(-\frac{\bar{r}}{|\bar{r}|}\cdot\bar{y}_2) - f(|\bar{r}|)(-\frac{\bar{r}}{|\bar{r}|}\cdot\bar{y}_2) + \mu(|\bar{r}|)\bar{x}_1\cdot\bar{y}_2 \end{aligned} \tag{2.4}$$

In the above control law the functions, $\mu(.)$, $f(.)$ and $\eta(.)$ are Lipschitz continuous. Also, $f(.)$ satisfies the following condition.

$$\begin{aligned} &\lim_{\rho\to 0} f(\rho) = \infty \\ &\lim_{\rho\to 0}\int_{\tilde{\rho}}^{\rho} f(\hat{\rho})d\hat{\rho} = \infty, \text{ for some } \tilde{\rho} > 0 \end{aligned} \tag{2.5}$$

In the above control law, u_1 and u_2.

1. The term $\mu(|\mathbf{r}|)\mathbf{x}_2\cdot\mathbf{y}_1$ and $\mu(|\mathbf{r}|)\mathbf{x}_1\cdot\mathbf{y}_2$ respectively tries to drive the system to a common orientation.

2. The terms with $f(.)$ are very important to prevent collision between the two UAVs and to achieve an appropriate separation.

3. The term $\mu(.)$ tries to align both the UAVs in either a parallel or a horizontal orientation.

The afore mentioned control law is elegant in the sense that it also helps reduce the dynamics of the combined system of two UAVs into the variables important for our formation problem. We can realise this by looking at the following transformations

$$\begin{aligned} \bar{r} &= |\bar{r}|ie^{i\Psi} = \bar{r}_2 - \bar{r}_1 \\ \bar{x}_1 &= e^{i\theta_1} \\ \bar{x}_2 &= e^{i\theta_2} \\ \phi_1 &= \theta_1 - \Psi \\ \phi_2 &= \theta_2 - \Psi \\ \rho &= |\bar{r}| \end{aligned} \tag{2.6}$$

Using these transformations, we get the following relations for $\dot{\rho}$, $\dot{\Psi}$, $\dot{\theta}_1$ and $\dot{\theta}_2$

$$\begin{aligned} \dot{\rho} &= \sin\phi_2 - \sin\phi_1 & \dot{\theta}_1 &= u_1 = -\eta(\rho)\sin\phi_1\cos\phi_1 + f(\rho)\cos\phi_1 + \mu(\rho)\sin(\theta_2 - \theta_1) \\ \dot{\Psi} &= -\frac{1}{\rho}(\cos\phi_2 - \cos\phi_1) & \dot{\theta}_2 &= u_2 = -\eta(\rho)\sin\phi_2\cos\phi_2 + f(\rho)\cos\phi_2 + \mu(\rho)\sin(\theta_1 - \theta_2) \end{aligned} \tag{2.7}$$

Since, $\phi_1 = \Psi - \theta_1$ and $\phi_2 = \Psi - \theta_2$. We can just reduce the dynamics of this combined system in terms of just three variables, (ρ, ϕ_1, ϕ_2)

$$\begin{aligned} \dot{\rho} &= \sin\phi_2 - \sin\phi_1 \\ \dot{\phi}_1 &= -\eta(\rho)\sin\phi_1\cos\phi_1 + f(\rho)\cos\phi_1 + \mu(\rho)\sin(\phi_2 - \phi_1) + \frac{1}{\rho}(\cos\phi_2 - \cos\phi_1) \\ \dot{\phi}_2 &= -\eta(\rho)\sin\phi_2\cos\phi_2 + f(\rho)\cos\phi_2 + \mu(\rho)\sin(\phi_1 - \phi_2) + \frac{1}{\rho}(\cos\phi_2 - \cos\phi_1) \end{aligned} \tag{2.8}$$

To check for stability consider the following candidate function

$$V(\rho, \phi_1, \phi_2) = -\log(cos(\phi_1 - \phi_2) + 1) + h(\rho) \tag{2.9}$$

Notice thatr Here, $\frac{dh(\rho)}{d\rho}(\rho) = f(\rho)$. Due to the proposed structure of $f(\rho)$ as given by 2.5 and the fact that $-\log(cos(\phi_1 - \phi_2) + 1) = 0$ at $(\phi_1 - \phi_2) = \pi/2$. This function indeed turns out to be positive and zero at equilibirium point. Notice that this Lyapunov function is only valid for all the points where $|\phi_1 - \phi_2| \neq \pi$

$$\Lambda = \{(\rho, \phi_1, \phi_2) || \phi_1 - \phi_2| \neq \pi \text{ and } 0 < \rho < \infty\} \tag{2.10}$$

To prove the stability of the control law, we need to show that the time derivative of this Lyapunov function is negative semi-definite.

$$\begin{aligned} V(\rho, \dot{\phi}_1, \phi_2) &= \frac{\sin(\phi_1 - \phi_2)}{1 + \cos(\phi_1 - \phi_2)}(\dot{\phi}_2 - \dot{\phi}_1) + f(\rho)\dot{\rho} \\ &= \frac{\sin(\phi_1 - \phi_2)}{1 + \cos(\phi_1 - \phi_2)}[-\eta(\rho)(\sin\phi_1\cos\phi_1 - \sin\phi_2\cos\phi_2) - f(\rho)(\cos\phi_1 + \cos\phi_2) \\ &+ \mu(\rho)((\sin(\phi_2 - \phi_1) - \sin(\phi_1 - \phi_2)))] + f(\rho)(\sin(\phi_2) - \sin(\phi_1)) \end{aligned} \tag{2.11}$$

Using the identity, $\sin(\phi_2 - \phi_1)(\cos(\phi_2) + \cos(\phi_1)) - (\cos(\phi_2 - \phi_1) + 1)(\sin\phi_2 - \sin\phi_1) = 0$, we get the following

$$V(\rho, \dot{\phi}_1, \phi_2) = -\frac{1}{\cos(\phi_1 - \phi_2) + 1}[\sin(\phi_1 - \phi_2)(2\mu(\rho)\sin(\phi_1 - \phi_2)) + \eta(\rho)/2(\sin(2\phi_1) - \sin 2\phi_2)]$$

Provided as long as we choose $2\mu(\rho) > \eta(\rho)$, we can easily prove stability using the following identity

$$\begin{aligned} \sin(\phi_2 - \phi_1)(\sin(\phi_2 - \phi_1) + \frac{1}{2}(\sin(2\phi_2) - \sin(2\phi_1))) = \frac{1}{2}[(\cos(\phi_1) + \cos(\phi_2))^2(\sin\phi_1 - \sin\phi_2)^2 \\ + (\sin^2\phi_1 - \sin^2\phi_2)^2] \end{aligned}$$

. This proves that $V(\rho, \dot{\phi}_1, \phi_2) \leq 0$. Using the Lasalle's Invariance principle, we can show that the largest invariant set, M is as given below

$$M = \{(\rho, \frac{\pi}{2}, \frac{\pi}{2}),\ \forall\rho\} \cup \{(\rho, -\frac{\pi}{2}, -\frac{\pi}{2}),\ \forall\rho\} \cup \{(\rho_o, 0, 0),\ f(\rho_0) = 0\} \cap \Omega$$

wherein Λ is as defined above in 2.10

As pointed out ealier the Lyapunov candidate function in this case fails to analyse equilibirum for all types of initial conditions. In order to analyse this system as a whole, we need pursue a general and co-ordinate free approach which is presented in the next section, wherein it is shown that each configuration of a single UAV can be represented in a compact form using a SE(2) Lie group representation.

2.1.2 Co-ordinate free approach

Any point, $(\bar{x}, \bar{y}, \bar{r})$ in the state space of a UAV can be represented with the following matrix group structure.

$$g = \begin{bmatrix} \bar{x} & \bar{y} & \bar{r} \\ 0 & 0 & 1 \end{bmatrix} \tag{2.12}$$

Since, $\bar{x}$ and $\bar{y}$ is a unit tangent and normal vectors, and $\bar{r}$ represents the inertial position of the UAV. This matrix structure has a Special Euclidean form(SE(2))

For a system of two UAVs with $g_1 = \begin{bmatrix} \bar{x}_1 & \bar{y}_1 & \bar{r}_1 \\ 0 & 0 & 1 \end{bmatrix}$, $g_2 = \begin{bmatrix} \bar{x}_2 & \bar{y}_2 & \bar{r}_2 \\ 0 & 0 & 1 \end{bmatrix}$ fo rms the following configuration manifold.

$$M_{config} = \{(g_1, g_2) \in SE(2) \times SE(2) | \mathbf{r}_1 \neq \mathbf{r}_2\}$$

The dynamics of each of this UAV can be represented as follows,

$$\begin{aligned} \dot{g}_1 &= g_1 \xi_1 = g_1(A_0 + A_1 u_1) \\ \dot{g}_2 &= g_2 \xi_2 = g_2(A_0 + A_1 u_2) \end{aligned} \tag{2.13}$$

Where, $\xi_1, \xi_2 \in \mathfrak{g}$ is the Lie algebra of G, and the matrices A_0 and A_1 are as follows,

$$A_0 = \begin{bmatrix} 0 & 0 & 1 \\ 0 & 0 & 0 \\ 0 & 0 & 0 \end{bmatrix} \quad A_1 = \begin{bmatrix} 0 & -1 & 0 \\ -1 & 0 & 0 \\ 0 & 0 & 0 \end{bmatrix} \tag{2.14}$$

We can represent the configuration of the first UAV with respect to other with the following transformation. This transformation turns out to be important to reduce the dynamics of this body UAV system.

$$g = g_1^{-1} g_2 \tag{2.15}$$

$$g = \begin{bmatrix} \bar{x}_1^T & -\bar{r}_1 \cdot \bar{x}_1 \\ \bar{y}_2^T & -\bar{r}_1 \cdot \bar{y}_1 \\ 0 \quad 0 & 1 \end{bmatrix} \begin{bmatrix} \bar{x}_2 & \bar{y}_2 & \bar{r}_2 \\ 0 & 0 & 1 \end{bmatrix} = \begin{bmatrix} \bar{x}_1 \cdot \bar{x}_2 & \bar{x}_1 \cdot \bar{y}_2 & (\bar{r}_2 - \bar{r}_1) \cdot \bar{x}_1 \\ \bar{y}_1 \cdot \bar{x}_2 & \bar{y}_1 \cdot \bar{y}_2 & (\bar{r}_2 - \bar{r}_1) \cdot \bar{y}_1 \\ 0 & 0 & 1 \end{bmatrix} \tag{2.16}$$

Similarly, we have the inverse as follows,

$$g_{-1} = g_2^{-1} g_1 = \begin{bmatrix} \bar{x}_2 \cdot \bar{x}_1 & \bar{x}_2 \cdot \bar{y}_1 & (\bar{r}_2 - \bar{r}_1) \cdot \bar{x}_1 \\ \bar{y}_2 \cdot \bar{x}_1 & \bar{y}_2 \cdot \bar{y}_1 & (\bar{r}_2 - \bar{r}_1) \cdot \bar{y}_1 \\ 0 & 0 & 1 \end{bmatrix} \tag{2.17}$$

From equations 2.16 and 2.17 we have the following mathematical relations, [1]

$$\begin{aligned} r &= \sqrt{g_{13}^2 + g_{23}^2} = \sqrt{(g^{13})^2 + (g^{23})^2} \\ g_{11} &= g_{22} = g^{11} = g^{22} \\ g_{12} &= -g_{21} = g^{21} = -g^{12} \\ 1 &= g_{11}^2 + g_{12}^2 \end{aligned} \tag{2.18}$$

Similarly, the control law can also be written in terms of g and g_{-1} as follows,

$$\begin{aligned} u_1(g) &= -\eta(r)\left(\frac{g_{13} g_{23}}{r^2}\right) + f(r)\left(\frac{g_{23}}{r}\right) + \mu(r) g_{21} \\ u_2(g) &= -\eta(r)\left(\frac{g^{13} g^{23}}{r^2}\right) + f(r)\left(\frac{g^{23}}{r}\right) + \mu(r) g^{21} \end{aligned} \tag{2.19}$$

[1] g_{ij} is an element of g and g^{ij} belongs to g^{-1}

From equations 2.15, 2.13 and 2.19 we get the following reduced G-invariant dynamics,

$$\dot{g} = -g_1^{-1}\dot{g}_1 g_1^{-1} g_2 + g_1^{-1}\dot{g}_2 = g\xi \tag{2.20}$$

Where, $\xi = \xi_2 - Ad_{g^{-1}}\xi_1$. The equilibrium of this combined system is just $\dot{g} = 0$. We get,

$$\xi(g_e) = \xi_2(g_e) - g_e^{-1}\xi_1(g_e)g_e = 0 \Rightarrow \xi_2(g_e)g_e^{-1} = g_e^{-1}\xi_1(g_e) \tag{2.21}$$

Solving, this we get,

$$\begin{aligned} u_2 &= u_1 \\ g_{11} &= 1 - g^{23}u_2 \\ g_{12} &= g^{13}u_1 \end{aligned} \tag{2.22}$$

Simplifying this above set of equations, we get the following relations,

$$\begin{aligned} 1 &= (1 - g_{23}u_1)^2 + g_{13}^2 u_1^2 \\ 0 &= u_1[(g_{13}^2 + g_{23}^2)u_1 - 2g_{23}] \\ u_1 &= 0 \quad u_1 = \tfrac{2g_{23}}{g_{13}^2 + g_{23}^2} \end{aligned} \tag{2.23}$$

If $u_1 = 0$ then we get $u_2 = 0$. We thus, get $\bar{x}_1 = \bar{x}_2$. If $u_2 = u_1 = 2g_{23}/r^2$. This suggests that UAVs converge to a circular trajectory in the state space.. This is illustrated in the figure 2.3.

In the next section we review the leader-follower planar formation strategy for a system of two AUVs (Autonomous Underwater Vehicles) using virtual structure based approach., [11]. In this article, the follower only gets the position measurement of the leader and has no idea about it's velocity or control model of the AUV. This is what motivated the authors to go for a virtual structure based approach for this system of two AUVs. The virtual structure approach creates a reference vehicle from the position measurement of the leader and using this particular reference vehicle a virtual vehicle is designed so that the follower may attain the position of this virtual vehicles. The virtual vehicle is designed in such a way that it converges to the reference and hence attaining a leader-follower formation at infinite time [4].

2.2 Virtual Structure Approach

We define the dynamics of the AUV in it's body fixed frame by the following equation(s).

$$\begin{aligned} M\dot{\nu} + C(\nu)\nu + D(\nu)\nu + g(\eta) &= \tau + \omega \\ \dot{\eta} &= R(\Psi)\nu \end{aligned} \tag{2.24}$$

where,$\nu - [u, v, r]$ and $\eta = [x, y, \phi]$ are generalized velocity and position of the AUV., M, $C(\eta)$ and $D(\eta)$ are Inertia, Coriolis, Centripetal forces respectively, $g(\eta)$ the buyoancy and gravitational forces and moments and τ is the input torques to this system and finally ω represent the bounded distrubances and $R(\Psi)$ is as follows,

$$R(\Psi) = \begin{bmatrix} \cos(\Psi) & -\sin(\Psi) & 0 \\ \sin(\Psi) & \cos(\Psi) & 0 \\ 0 & 0 & 1 \end{bmatrix} \tag{2.25}$$

2.2.1 Design of Virtual Vehicle

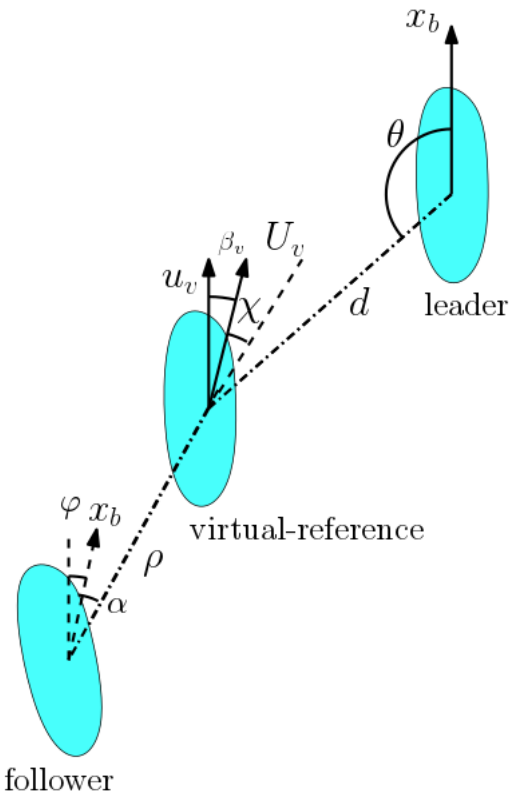

Figure 2.4: Reference vehicle design

As shown in the figure 2.4, the reference vehicle is to be kept at a distance of d from the leader. Note that we designate the leader, reference, virtual, follower by the symbols,m, r, v, f respectively. We define the the position and dynamics of the reference vehicle as follows,

$$\begin{aligned} \eta_r &= \eta_m + R(\Psi_m) \begin{bmatrix} d\cos(\theta) \\ d\sin(\theta) \\ 0 \end{bmatrix} \\ \dot{\eta}_r &= R(\Psi_m) v_r \end{aligned} \tag{2.26}$$

where, $v_r = [u_m - d\cos(\theta)r_m, v_m - d\sin(\theta)r_m, r_m]$
Based on the reference vehicle trajectory (2.26), we define the virtual vehicle dynamics as follows,

$$\dot{\eta}_v = R(\Psi_v)v_v \tag{2.27}$$

where, $v_v = R^{-1}(\Psi_v)(\beta_1(\phi) + \beta_2(\phi))$ and $\beta_1(\phi) = [\lambda_1 tanh(\phi_1/\lambda_1), \lambda_2 tanh(\phi_2/\lambda_2), \lambda_3 tanh(\phi_3/\lambda_3)]$ and $\beta_2(\phi) = [k_1 tanh(\phi_1/k_1), k_2 tanh(\phi_2/k_2), k_3 tanh(\phi_3/k_3)]$ and $\phi = [\phi_1, \phi_2, \phi_3]$ and
$\dot{\phi} = -\beta_1(\phi) - diag(k_1, k_2, k_3)(\eta_v - \eta_r + \phi)$.
It is further shown that the this virtual vehicle is Uniform Semiglobal Practical Asymptotic Stable (USPAS)[2] by considering the Lyapunov candidate function as follows,

$$V_e(t) = \frac{1}{2} r_e^T r_e + \phi_1 ch^T \phi_{ch} \tag{2.28}$$

where, $\phi_{ch} = [\sqrt{k_1 \log(\cosh(\phi_1/k_1))}, \sqrt{k_2 \log(\cosh(\phi_2/k_2))}, \sqrt{k_3 \log(\cosh(\phi_3/k_3))}]$. It turns out that we can stabilize our system for $\|r_e\| < \epsilon$ for any $\epsilon > 0$ by selecting appropriate gains, i.e $\dot{V}_e \leq 0$ for $\|r_e\| < \epsilon$.
Using velocity information from this virtual vehicle, we now design a position tracking control for the follower. We perform the following transformations,

$$\begin{aligned} \rho &= \sqrt{(x_v - x_f)^2 + (y_v - y_f)^2} \\ x_f - x_v &= -\rho\cos(\varphi + \alpha) \\ y_f - y_v &= -\rho\sin(\varphi + \alpha) \\ \varphi + \alpha &= arctan(\frac{y_v - y_f}{x_v - x_f}) \end{aligned} \tag{2.29}$$

Using this transformations, the dynamics turn out to be as follows,

$$\begin{aligned} \dot{\rho} &= -u_f\cos(\alpha) - v_f\sin(\alpha) + U_v\cos(\chi) \\ \dot{\alpha} &= \frac{\sin(\alpha)}{\rho}u_f - \frac{\cos(\alpha)}{\rho}v_f - r_f - U_v\frac{\sin(\chi)}{\rho} \end{aligned} \tag{2.30}$$

where, χ is as shown in figure 2.4

2.2.2 Kinematic Control

Since, the velocities of the AUV is passively controlled via equation 2.24. It is possible to regulate r_f such that $\alpha \to 0$. By using this simple feedback law,

$$r_f = \frac{\sin(\alpha)}{\rho}u_f - \frac{\cos(\alpha)}{\rho}v_f - U_v\frac{\sin(\chi)}{\rho} + K_4\alpha \tag{2.31}$$

where, $K_4 > 0$ it can be easily shown that $\lim_{t\to\infty} \alpha = 0$ by taking the candidate Lyapunov function $V_1 = \alpha^2/2$
Considering the dynamics 2.30 as a cascaded system. We design the control u_f based on the nominal form for these equations as follows,

$$\begin{aligned} \dot{\rho} &= -u_f + U_v \cos(\chi) \\ u_f &= K_5\bar{\rho} + U_v \cos(\chi) \end{aligned} \tag{2.32}$$

where, $\bar{\rho} = \rho - \delta$ and $K_5 > 0$ Using the expressions for u_f and r_f we can express the closed loop dynamics of v_f as follows,

$$\dot{v}_f = -h_1(.)v_f + h_2(.)\rho + h_3(.) + \omega_2' \tag{2.33}$$

where, h_1, h_2, h_3 are some function of state space. It can be shown that, $\lim_{t\to\infty} \bar{\rho} = 0$ using the following candidate Lyapunov function,

$$V_1(\rho, v_f) = \frac{1}{2}\rho^2 + \frac{1}{2}v_f^2 \tag{2.34}$$

2.2.3 Dynamic Control

For Dynamic control of the follower AUV. Consider the following error variable, $z_1 = u_f - \alpha_u$ and $z_2 = r_f - \alpha_r$.where, u_f and r_f be the virtual control inputs respectively, and α_u and α_r be the corresponding virtual controls. It can be shown that ($\bar{\rho} \to 0$, $v_f \to 0$,$z_1 \to 0$ $z_2 \to 0$) using the following candiate Lyapunov function

$$V_2 = \frac{1}{2}\bar{\rho}^2 + \frac{1}{2}v_f^2 + \frac{1}{2}m_{11}z_1^2 + \frac{1}{2}m_{33}z_2^2 \tag{2.35}$$

In the next chapter, we propose a control law for a system of two Purcell's swimmer which attains a circular formation. We later go on to show it's stability using the Lyapunov function approach. We also show a leader-follower type of formation for a two-agent Purcell swimmer and prove its stability using the first principles.

Chapter 3

Purcell's Formation Control problem

In this chapter we talk about two different types of formation for a pair of Purcell swimmers. In this first formation, we have these two swimmers arbitarily initialised and the job of the controller designers like us would be formulate a control strategy in order for these two swimmers to start circulating around a common center.
The ideas of a circular formation is built upon in the section after that wherein, we again have two Purcell's swimmers but the first swimmer(leader swimmer) is moving on a trajectory that is smooth but unknown to the second swimmer(follower swimmer) and job of control design is to come up with a control strategy to keep up with the leader at a fixed relative orientation.
Before we begin this section there are some notational freedom that we have undertaken to make the math look simpler to understand.

1. All the two side angles of any one the swimmer is represented as, $\alpha = (\alpha_1, \alpha_2)$
2. Even the two control inputs of each of the swimmer will be represented in a vectorised form, $U = (u_1, u_2)$

3.1 Circular formation

In this section we first talk about the kinematic equations of the Purcell swimmer that we are going to be working with. We then talk in-depth about the circular formation that we wish to achieve using a two-agent Purcell's swimmer. There are many questions that arises when one talks about a circular formation.

The rationale behind choosing a circular formation for the co-ordination problem was to understand fully the non-linearities in the Purcell swimmers kinematic equations. A simple leader-follower behavior then becomes a simple extension to this problem definition

3.1.1 The Purcell swimmer

The kinematic equations for each Purcell swimmer [7] as shown in the figure 3.1 is as follows,

$$\begin{bmatrix} \dot{x} \\ \dot{y} \\ \dot{\theta} \\ \dot{\alpha}_1 \\ \dot{\alpha}_2 \end{bmatrix} = \begin{bmatrix} A(\alpha) \\ I \end{bmatrix} \begin{bmatrix} u_1 \\ u_2 \end{bmatrix} \tag{3.1}$$

where, $\alpha = (\alpha_1, \alpha_2)$ and α_1, α_2 represent each of the side angle of the Purcell swimmer.

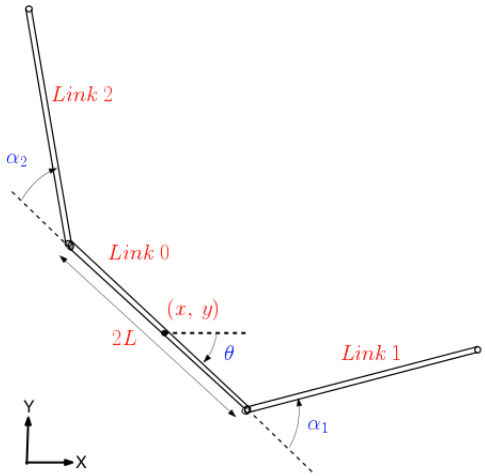

Figure 3.1: Schematic of the Purcell's swimmer

$u_1 = \dot{\alpha}_1$ and $u_2 = \dot{\alpha}_2$ are the control inputs to the system and $A(\alpha)$ is the mapping from the shape velocity, $(\dot{\alpha}_1, \dot{\alpha}_2)$ to group velocity$(\dot{x}, \dot{y}, \dot{\theta})$. Note that in these equations above, $\dot{x}$ and $\dot{y}$ are the velocity in the local co-ordinate system, i.e $\dot{x}$ is along the middle link and $\dot{y}$ is perpendicular to the middle link.

To solve the co-ordination control problem, we need these kinematic set of equations in an inertial frame of reference. As it turns out, we can indeed convert these kinematic

set of equations to an inertial one using a simple transformation as under,

$$\begin{bmatrix} \dot{X} \\ \dot{Y} \\ \dot{\theta} \\ \dot{\alpha}_1 \\ \dot{\alpha}_2 \end{bmatrix} = \begin{bmatrix} R(\theta)A(\alpha) \\ I \end{bmatrix} \begin{bmatrix} u_1 \\ u_2 \end{bmatrix} \tag{3.2}$$

$$R(\theta) = \begin{bmatrix} \cos(\theta) & -\sin(\theta) & 0 \\ \sin(\theta) & \cos(\theta) & 0 \\ 0 & 0 & 1 \end{bmatrix}$$

Note that in this case, $\dot{X}$ is aligned along the inertial x-axis and $\dot{Y}$ is the direction representing y-axis as shown in the figure 3.1

3.1.2 Circular Formation

For a formation control problem in this particular case, we have two such Purcell's swimmers and we wish to come up with a control strategy such that these two swimmers start executing a circular trajectory around a common center with the diameter being R_0. Now, for a two-swimmer system to start executing a circular formation without some information about the other swimmer is just not possible. In this particular problem, each of these swimmer have the information about the radial separation(ρ) between the other swimmer as well as the angular orientation of this other swimmer with respect to itself(ϕ_2). This can be clearly seen in the figure **??**. Using these these external information variables along with the swimmers' internal variables like α_1, α_2 each of the swimmer is supposed to come up with an control formulation such that the swimmers start executing a circular formation with the diameter equal to R_0 and the angular velocity of 1 with respect to other swimmer.

It is important to note here that with this information variables it is not possible to ensure that the center of this circular formation to be a stationary point. This is due to the fact using the ρ, ϕ_2 information it is not possible to extract information about the relative orientation of the two swimmers with respect to each other. This won't allow us to know whether the velocities vectors of each of the swimmers are anti-parallel to each other which in-turn won't allow the swimmers to execute a circular formation around a stationery point.

3.1.3 Transformations

In this section, we talk about the transformations that are necessary to understand the control strategy for a circular formation of the Purcell swimmer.

Let the position of each of the Purcell swimmer(abbreviated as 1 and 2 respectively) be $\bar{r}_1$ and $\bar{r}_2$ respectively. Thus, we have the following relationship between $\bar{r}_1, \bar{r}_2, \rho, \phi_1$.

$$\bar{r}_2 - \bar{r}_1 = \rho(\cos(\phi_2)\hat{i} + \sin(\phi_2)\hat{j}) \tag{3.3}$$

where, $\hat{i}$ and $\hat{j}$ are unit vectors along X and Y axis respectively. Time derivative of the above equation yields us the following relation

$$\begin{aligned} \dot{\rho} &= [\cos(\phi_2) \quad \sin(\phi_2)] \cdot (\dot{\bar{r}}_2 - \dot{\bar{r}}_1) \\ \dot{\phi}_2 &= \frac{1}{\rho}[-\sin(\phi_2) \quad \cos(\phi_2)] \cdot (\dot{\bar{r}}_2 - \dot{\bar{r}}_1) \end{aligned} \tag{3.4}$$

In the context of the Purcell swimmer 3.2, $\dot{\bar{r}}_1$ and $\dot{\bar{r}}_2$ can be written down as follows,

$$\begin{aligned} \dot{\bar{r}}_1 &= \begin{bmatrix} \cos(\theta_1) & -\sin(\theta_1) \\ \sin(\theta_1) & \cos(\theta_1) \end{bmatrix} (A(\alpha_{\mathbf{1}})_{2\times 2})U_1 \\ \dot{\bar{r}}_2 &= \begin{bmatrix} \cos(\theta_2) & -\sin(\theta_2) \\ \sin(\theta_2) & \cos(\theta_2) \end{bmatrix} (A(\alpha_{\mathbf{2}}))_{2\times 2}U_2 \end{aligned} \tag{3.5}$$

where, $A(\alpha)_{2\times 2}$ corresponds to the first two rows of the $A(\alpha)$. $\alpha_{\mathbf{1}} = (\alpha_{11}, \alpha_{12})$ corresponds to both the link angles of the first swimmer and $\alpha_{\mathbf{2}} = (\alpha_{21}, \alpha_{22})$ corresponds to both the angles of the second swimmer. Also, $U_1 = (u_{11}, u_{12})$ and $U_2 = (u_{21}, u_{22})$ corresponds to the control inputs for each of the swimmer.

Substituting 3.5 in equation 3.4 and simplifying the equations we get the following results, (Note: $\phi_2 = \phi_1 + \pi$)

$$\begin{aligned} \dot{\rho} = {} & [\cos(\theta_2 - \phi_2) \quad -\sin(\theta_2 - \phi_2)](A(\alpha_2)_{2\times 2})U_2 \\ & + [\cos(\theta_1 - \phi_1) \quad -\sin(\theta_1 - \phi_1)](A(\alpha_2))_{2\times 2})U_1 \end{aligned} \tag{3.6}$$

$$\begin{aligned} \dot{\phi}_1 = \frac{1}{\rho}(& [\sin(\theta_2 - \phi_2) \quad \cos(\theta_2 - \phi_2)](A(\alpha_2)_{2\times 2})U_2 \\ & + [\sin(\theta_1 - \phi_1) \quad \cos(\theta_1 - \phi_1)](A(\alpha_1)_{2\times 2})U_1) \end{aligned} \tag{3.7}$$

3.1.4 Control Law

For attaining the circular formation, we propose the following control law

$$U_1 = K_r(R_0 - \rho)\begin{bmatrix} \sin(\psi_1(\alpha_{\mathbf{1}}) - \Omega_1) \\ \sin(\psi_2(\alpha_{\mathbf{1}}) - \Omega_1) \end{bmatrix} + K(\alpha_{\mathbf{1}})\begin{bmatrix} -\Lambda_2(\alpha_{\mathbf{1}})\sin(\psi_2(\alpha_{\mathbf{1}}) - \Omega_1) \\ \Lambda_1(\alpha_{\mathbf{1}})\sin(\psi_1(\alpha_{\mathbf{1}}) - \Omega_1) \end{bmatrix} \tag{3.8}$$

$$U_2 = K_r(R_0 - \rho)\begin{bmatrix}\sin(\psi_1(\alpha_2) - \Omega_2)\\ \sin(\psi_2(\alpha_2) - \Omega_2)\end{bmatrix} + K(\alpha_2)\begin{bmatrix}-\Lambda_2(\alpha_2)\sin(\psi_2(\alpha_2) - \Omega_2)\\ \Lambda_1(\alpha_2)\sin(\psi_1(\alpha_2) - \Omega_2)\end{bmatrix} \tag{3.9}$$

Where, $\Omega_1 = \theta_1 - \phi_1$ and $\Omega_2 = \theta_2 - \phi_2$
K_r is a positive constant

$$\begin{aligned}\Lambda_i(\alpha) &= \sqrt{A_{1i}^2(\alpha) + A_{2i}(\alpha)^2}\\ \sin(\Psi_i(\alpha)) &= \frac{A_{1i}(\alpha)}{\Lambda_i(\alpha)}\\ \cos(\Psi_i(\alpha)) &= \frac{A_{2i}(\alpha)}{\Lambda_i(\alpha)}\end{aligned} \tag{3.10}$$

where, $i \in \{1, 2\}$

$$K(\alpha) = \frac{1}{2}\left(\frac{R_0}{\Lambda_1(\alpha)\Lambda_2(\alpha)\sin(\Psi_1(\alpha)) - \Psi_2(\alpha)}\right) \tag{3.11}$$

To get an intuition behind the terms like $\Lambda_1(\alpha), \Psi_1(\alpha), \Psi_2(\alpha)$. Consider the kinematic equation of the Purcell swimmer as shown in equation 3.1 with $u1 = u$ and $u_2 = 0$.

$$\begin{bmatrix}\dot{x}\\ \dot{y}\end{bmatrix} = A_1(\alpha)u \tag{3.12}$$

where, $A_1(.)$ is the first column of the A matrix. Using 3.10 we can re-write this column as follows,

$$\begin{bmatrix}\dot{x}\\ \dot{y}\end{bmatrix} = \Lambda_1(\alpha)\begin{bmatrix}\sin(\Psi_1(\alpha))\\ \cos(\Psi_1(\alpha))\end{bmatrix}u \tag{3.13}$$

So a better understanding of the $\Psi_1(\alpha)$ is that it gives us the direction in which the control u_1 maneuvers a system if $u_2 = 0$. A similar explaination follows for $\Psi_2(\alpha)$. Now, if we write the kinematic equations of the Purcell swimmer together, consider this form,

$$\begin{bmatrix}\dot{x}\\ \dot{y}\end{bmatrix} = \Lambda_1(\alpha)\begin{bmatrix}\sin(\Psi_1(\alpha))\\ \cos(\Psi_1(\alpha))\end{bmatrix}u_1 + \Lambda_2(\alpha)\begin{bmatrix}\sin(\Psi_2(\alpha))\\ \cos(\Psi_2(\alpha))\end{bmatrix}u_2 \tag{3.14}$$

There are two terms in the control law 3.8. The first term in each of these two control law is solely responsible behind attaining a radial separation of R_0. The second term however is used to generate an angular velocity in this two-agent swimmer.

Now, a natural question arises regarding the intuition behind this peculiar form of the control law. To get a better understanding, consider the following figure 3.2. Now, as mentioned by the equation 3.14 above the net direction of motion of one particular swimmer is the vector sum of the motion generated by each of the actuators in the Purcell swimmer. Now, the amount that each of control inputs contribute towards increasing or

decreasing the radial distance ρ depends upon the projection from the $\begin{bmatrix} \sin(\Psi_1(\alpha)) \\ \cos(\Psi_1(\alpha)) \end{bmatrix}$ on the $\begin{bmatrix} \cos(\Omega) \\ -\sin(\Omega) \end{bmatrix}$ vector. This projection may be positive or negative depending upon the angle between these two vectors.

Consider the case when, $\rho > R_0$ and the angle between each of the vectors mentioned above is obtuse. So, in this particular case the projection becomes negative which implies that the distance(ρ) will keep on increasing irrespective of the value of ρ. To keep this from happening we substitute u_1 by the value of the projection, i.e $\sin(\psi_1(\alpha) - \Omega)$ so that the actual value of the projection between turns out to be positive which we later later scale it by $K_r(R_0 - \rho)$ to ensure the correction direction of increase or decrease in ρ. It is important to note that whenever $\rho = R_0$ the first term vanishes. Thus, the second

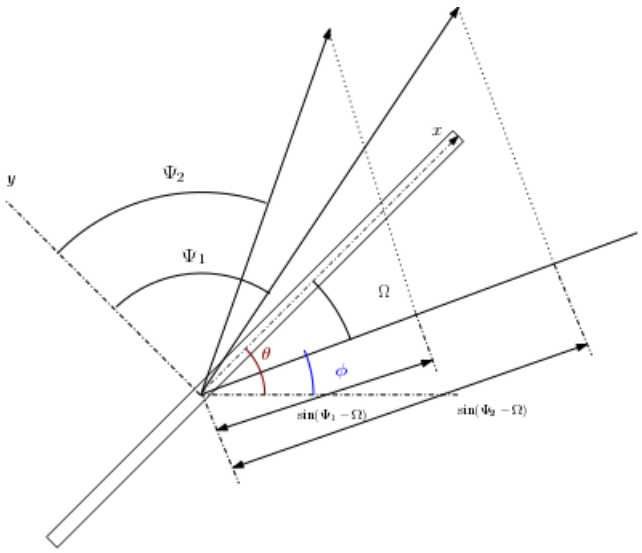

Figure 3.2: schematic of the terms in the control law

term was added such that it provides no contribution to the projection on the $\begin{bmatrix} \cos(\Omega) \\ -\sin(\Omega) \end{bmatrix}$ plus it helps in generating an angular velocity to the combined system.

A peculiar thing about this control law 3.8 is the fact that it helps reduce the no of variables to 7.

$$\begin{bmatrix} \dot{\rho} \\ \dot{\Omega}_1 \\ \dot{\Omega}_2 \\ \dot{\alpha}_1 \\ \dot{\alpha}_2 \end{bmatrix} = \begin{bmatrix} [\cos(\theta_2-\phi_2) \quad -\sin(\theta_2-\phi_2)](A(\alpha_2)_{2\times2})U_2 + [\cos(\theta_1-\phi_1) \quad -\sin(\theta_1-\phi_1)](A(\alpha_2))_{2\times2})U_1 \\ \frac{1}{\rho}([\sin(\theta_2-\phi_2) \quad \cos(\theta_2-\phi_2)](A(\alpha_2)_{2\times2})U_2 + [\sin(\theta_1-\phi_1) \quad \cos(\theta_1-\phi_1)](A(\alpha_1)_{2\times2})U_1) \\ A_3(\alpha_1)U_1 - \dot{\phi}_1 \\ A_3(\alpha_2)U_2 - \dot{\phi}_1 \\ U_1 \\ U_2 \end{bmatrix} \tag{3.15}$$

where, U_1 and U_2 are defined in 3.8 and $A_i(\alpha)$ represents the ith row in the A matrix.

3.1.5 Convergence

In order to prove stability of this control formulation we are currently using a Lyapunov's second theorem. Lyapunov's second theorem says that if you a have a positive definite function(say $V(x)$) as a function of your state space and you can show that the time derivative of this Lyapunov function is less than zero then it can be inferred that this function indeed goes to the equilibrium. In this particular problem we first show using Lyapunov's approach that the system indeed does tend to a radial separation of R_0. We later also show that as the system tends to a radial separation of R_0 the combined angular velocity of this two-agent system goes to 1.

In order to first demonstrate that the system indeed does tend to a radial separation of R_0, consider the following Lyapunov function

$$V(\rho,\phi,\theta_1,\theta_2,\alpha_1,\alpha_2) = \frac{1}{2}(\rho - R_0)^2 \tag{3.16}$$

the time derivative of this Lyapunov function is as follows,

$$\dot{V}(\rho,\phi,\theta_1,\theta_2,\alpha_1,\alpha_2) = 2(\rho - R_0)\dot{\rho} \tag{3.17}$$

Substituting the control law 3.8 in the kinematic transformation equation 3.6 we get $\dot{\rho}$ following,

$$\dot{\rho} = -K_r(\rho - R_0)(\sum_{i=0}^{i=1}\sum_{j=0}^{j=1}\Lambda_i(\alpha_j)\sin^2(\Psi_i(\alpha_j) - \Omega_j)) \tag{3.18}$$

Substituting this equation in derivative of Lyapunov function

$$\dot{V}(\rho,\phi,\theta_1,\theta_2,\alpha_1,\alpha_2) = -K_r(\rho - R_0)^2(\sum_{i=0}^{i=1}\sum_{j=0}^{j=1}\Lambda_i(\alpha_j)\sin^2(\Psi_i(\alpha_j) - \Omega_j)) \tag{3.19}$$

Since clearly $\dot{V}(\rho) \leq 0$ we need to use LaSalle's invariance principle to classify asymptotic stability which is stated as follows,[10]

Theorem 1. Let $\Theta \subset D \subset \mathbb{R}^n$ be a compact positively invariant set with respect to the system dynamics. Let $V\colon D \to R$ be a continuously differentiable function such that $\dot{V} \leq 0$ in Θ. Let $E \subset \Theta$ be the set of all points in where $\dot{V} = 0$. Let $M \subset E$ be the largest invariant set in E. Then every solution starting in Θ approaches M as $t \to \infty$

To use this theorem we first need to determine a compact positively invariant set which we claim to be $\Theta = \{(\rho, \alpha_1, \alpha_2, \Omega_1, \Omega_2) | V(\rho) \leq c\}$ for some $c > 0$. Since $\dot{V}(\rho) \leq 0$ any trajectory starting in Θ won't be able to exit this set due to negative semidefiniteness of $V(.)$ which makes the set compact as well as invariant. For this function, $\dot{V}(\rho, \phi, \theta_1, \theta_2, \alpha_1, \alpha_2) = 0$ spans the following set.

$$E = \{(\rho, \alpha_1, \alpha_2, \Omega_1, \Omega_2) | \rho = R_0\} \cup$$
$$\{(\rho, \alpha_1, \alpha_2, \Omega_1, \Omega_2) | \Omega_1 = \Psi_1(\alpha_1) = \Psi_2(\alpha_1), \Omega_2 = \Psi_1(\alpha_2) = \Psi_2(\alpha_2)\} \cap \Theta$$

Using LaSalle's invariance principle, we can determine the equilibirium of the system by determining the largest invariant set. To determine the largest invariant set, consider the definition of invariant set which states an invariant set is a set wherein a system which starts from any point in that set remains in that set even under the influence of the dynamical system.

To determine the Invariant set, consider the first set i.e, $E_1 = \{(\rho, \alpha_1, \alpha_2, \Omega_1, \Omega_2) | \rho = R_0\} \cap \Theta$. For trajectory, $\gamma(t)$ starting with $\gamma(0) \in E_1$ we always get $\dot{\rho} = 0$(3.15). This result implies as long as the trajectory starts in E_1 initial condition is $\dot{(\rho)} = 0$ over all the points in E_1. Thus, E_1 is an invariant set in itself.

Now consider the second set, $E_2 = \{(\rho, \alpha_1, \alpha_2, \Omega_1, \Omega_2) | \Omega_1 = \Psi_1(\alpha_1) = \Psi_2(\alpha_1), \Omega_2 = \Psi_1(\alpha_2) = \Psi_2(\alpha_2)\} \cap \Theta$. Using the definition of this set, if we substitute the value in the 3.15 we get,$(\dot{\rho}, \dot{\phi}, \dot{\theta_1}, \dot{\theta_2}, \dot{\alpha_1}, \dot{\alpha_2}) = (0, 0, 0, 0, 0, 0, 0, 0)$. Thus, again in this case any trajectory starting in E_2 will remain in E_2. Hence, by this argument even E_2 is an invariant set.

Thus, the largest Invariant set from the set of $\dot{V}(\rho) = 0$ is as follows,

$$M = E_1 \cup E_2$$

Let us now further talk about maybe a physical intuition behind these invariance. First consider the second invariant set,

$$E_2 = \{(\rho, \alpha_1, \alpha_2, \Omega_1, \Omega_2) | \alpha_1, \alpha_2 \in S, \Omega_1 = \Psi_1(\alpha_1), \Omega_2 = \Psi_1(\alpha_2)\} \tag{3.20}$$

where, $S = \{\alpha | \Psi_1(\alpha) = \Psi_2(\alpha)\}$ To get a better intuition of what this set represents consider the figure 3.2. If $\Psi_1(\alpha) = \Omega = \Psi_2(\alpha)$ this implies each of the control input, $U_1 = \dot{\alpha}_1$ is unable to project its direction of motion to aid in the increase or decrease in $\dot{\rho}$.

Thus, it cannot be used to generate the specified value of R_0.

In fact, it is also possible to determine the set S using symmetry operations in the dynamical model of the swimmer [6] which leads to the following claim.

$$S = \{(\alpha, -\alpha) | \quad \alpha \in [-\pi, \pi]\} \tag{3.21}$$

Proof. To show that this is indeed the solution to the equation $\Psi_1(\alpha, -\alpha) = \Psi_2(\alpha, -\alpha)$. Consider the axial and front-back symmetries in the Purcell swimmer [6] as follows,

$$\begin{aligned} A(-\alpha_1, \alpha_2) &= \begin{bmatrix} -1 & 0 & 0 \\ 0 & 1 & 0 \\ 0 & 0 & 1 \end{bmatrix} A(\alpha_1, \alpha_2) \\ A(\alpha_2, \alpha_1) &= \begin{bmatrix} -1 & 0 & 0 \\ 0 & 1 & 0 \\ 0 & 0 & -1 \end{bmatrix} A(\alpha_1, \alpha_2) \begin{bmatrix} 0 & 1 \\ 1 & 0 \end{bmatrix} \end{aligned} \tag{3.22}$$

If we substitute an element of set S as given 3.21 through the symmetry operations as mentioned in equation 3.22. We get the following,

$$\begin{bmatrix} -1 & 0 & 0 \\ 0 & 1 & 0 \\ 0 & 0 & 1 \end{bmatrix} A(\alpha, -\alpha) = \begin{bmatrix} -1 & 0 & 0 \\ 0 & 1 & 0 \\ 0 & 0 & -1 \end{bmatrix} A(\alpha, -\alpha) \begin{bmatrix} 0 & 1 \\ 1 & 0 \end{bmatrix} \tag{3.23}$$

The above algebra gives us the following required solution.

$$\begin{aligned} A_{11}(\alpha, -\alpha) &= A_{12}(\alpha, -\alpha) \\ A_{21}(\alpha, -\alpha) &= A_{22}(\alpha, -\alpha) \end{aligned} \Rightarrow \Psi_1(\alpha, -\alpha) = \Psi_2(\alpha, -\alpha)$$

This completes the proof. □

The findings of this claim has been verified by numerically solving $\Psi_1(\alpha) = \Psi_2(\alpha)$ which can be observed in figure 3.3.

The first equilibrium set, E_1 specifies the states that corresponds to the desired separation of R_0. This set is defined as follows,

$$E_1 = \{(\rho, \alpha_1, \alpha_2, \Omega_1, \Omega_2) | \rho = R_0\} \tag{3.24}$$

Our approach to determine the equilibrium is as follows, we first linearize our system about the set E_2. If we can show that every point in E_2 constitutes an unstable equilibrium then it can be concluded in an obvious way that any trajectory tends to the set E_2.
Since, E_2 is a continuum we discretise this set into a finite number of points and we

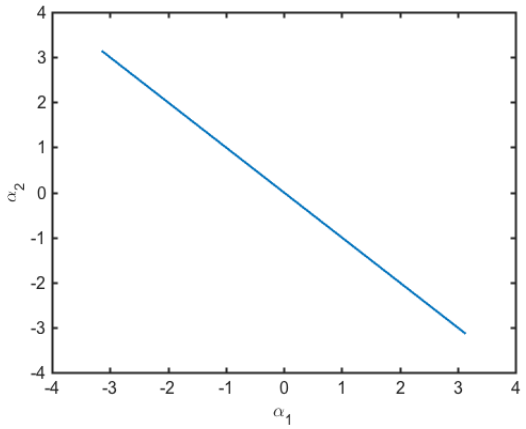

Figure 3.3: α such that $\Psi_1(\alpha) = \Psi_2(\alpha)$

checked for Eigen values at each of these points in the set E_2. It turns out that in all these cases there exists atleast one Eigen value whose real part is greater than zero which makes all of these points in E_2 unstable (theorem 4.7 [10]). Note that since we only checked for instability at a finite number of points in the set E_2 we still need to prove this result for all the points in these set which hasn't been proven till now.

The argument that the two-agent system will converge to the first equilibrium, E_1 simply follows from the argument that since the two-agent swimmer has to converge to one of the equilibirium points, E_1 or E_2. But since, E_2 turned out to be unstable, the system will indeed converge to a equilibirium separation of R_0, i.e the set E_1.

To show that the system indeed does converge to an angular velocity of 1 rad/s. We show that as the radial separation tends to R_0 the combined angular velocity tends to 1. When, $\rho \to R_0$ we get,

$$\begin{aligned}\dot{\phi_1} = \frac{1}{R_0}(K(\alpha_1)\Lambda_1(\alpha_1)\Lambda_2(\alpha_1)\sin(\psi_2(\alpha_1) - \psi_1(\alpha_1)) \\ + K(\alpha_2)\Lambda_1(\alpha_2)\Lambda_2(\alpha_2)\sin(\psi_2(\alpha_2) - \psi_1(\alpha_2))\end{aligned} \tag{3.25}$$

Substituting the value of $K(\alpha)$ as mentioned earlier we get,

$$\dot{\phi_2} = 1 \tag{3.26}$$

The result $\dot{\phi_2} = 1$ finally proves that this control law 3.8 does indeed converge to a fixed radial separation of R_0 and an angular velocity of 1 rad/s.

In conclusion, in this section we saw a control law that demonstrated the convergence of a two-agent swimmers which were arbitrarily initialized to a radial separation of R_0 and angular velocity of 1 rad/s. In the next section, we build up on this work to demonstrate a control formulation for a two-agent swimmer to demonstrate a leader-follower

type of behavior wherein the leader the moving along any predefined trajectory and the follower unaware of this trajectory is expected to attain a fixed geometrical configuration with respect to the leader.

3.2 Leader-Follower separation

Leader follower formation are the essence of formation control problems. This is due to the fact that any formation problem consisting of N different bodies can be divided into smaller Leader-Follower sub-problems to further solve the formation problem.

As explained earlier, In a leader-follower formation the leading swimmer is moving along a pre-defined trajectory, $\gamma(t)$ is the state space and the job of the follower is to attain a fixed geometrical configuration with respect to the leader without the prior knowledge about the leader's trajectory. This relative geometric configuration is highly dependent based on the information sharing protocol between the leader and the follower but in many cases this relative configuration is about maintaining fixed radial distance, ρ and the angular separation, ϕ between between the leader and the follower as shown in the figure 3.4. In this particular problem the geometric configuration that we are talking about in this case is to attain a fixed radial distance, R_0 and a fixed angular separation, ϕ_0.

Before moving ahead we are going to be assuming that the leader trajectory is upper bounded by V_{max}. To actually get an understanding of what we mean by the last statement consider a scenario wherein leader swimmer is following the trajectory, $\gamma(t) = (t, t^2)$. So the velocity of this swimmer, $\gamma'(t) = (1, 2t)$. It is very clear from looking at $\gamma'(t)$ that the velocity of the leader keeps on increasing as $t \to \infty$. This means that in order to keep up with this trajectory we need to apply an infinite amount of control actuation to the follower. Since, it is not practical solution to apply an infinite amount of control we are going ahead with a simple assumption that, we keep the norm of the velocity of the leader bounded which has been stated below.

Assumption 1. *The magnitude of velocity of the leader at any point of time is bounded*

$$||\gamma'(t)||_2 \leq V_{max} \quad \forall t \geq 0 \tag{3.27}$$

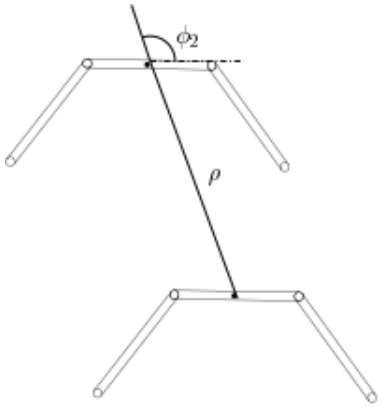

Figure 3.4: Schematic of a Leader-follower behavior

3.2.1 Control Law

$$U_F = \begin{bmatrix} \frac{\cos(\Psi_2-\Omega)}{\Lambda_1 \sin(\Psi_1-\Psi_2)} \\ -\frac{\cos(\Psi_1-\Omega)}{\Lambda_2 \sin(\Psi_1-\Psi_2)} \end{bmatrix} K_r(R_0-\rho) - K_V sgn(R_0-\rho) + \\ \begin{bmatrix} \frac{\sin(\Psi_2-\Omega)}{\Lambda_1 \sin(\Psi_1-\Psi_2)} \\ -\frac{\sin(\Psi_1-\Omega)}{\Lambda_2 \sin(\Psi_1-\Psi_2)} \end{bmatrix} K_\phi(\phi_0-\phi) - K_V sgn(\phi_0-\phi) \tag{3.28}$$

where, Ψ_i, Λ_i is as defined in equation 3.10, $\Omega = \theta_F - \phi$ and $sgn(.)$ is the signum function and $K_V > V_{max}$

Note that there are two terms in the control law 3.28. The first term which consists entirely of ρ terms helps in attaining a radial separation of R_0. Second term consists entirely of ϕ helps in attaining the fixed angular orientation ϕ_0.

To understand the term $\begin{bmatrix} \frac{\cos(\Psi_2-\Omega)}{\Lambda_1 \sin(\Psi_1-\Psi_2)} \\ \frac{\cos(\Psi_1-\Omega)}{\Lambda_2 \sin(\Psi_1-\Psi_2)} \end{bmatrix}$ term. We know that the projection of u_1 on the ρ axis is $\sin(\Psi_1 - \Omega)$ and similarly u_2 is $\sin(\Psi_2 - \Omega)$. Thus, the value of $\dot{\rho} = \Lambda_1 \sin(\Psi_1 - \Omega)u_1 + \Lambda_2 \sin(\Psi_2 - \Omega)u_2$. If we substitute the first term in the control law gives us a unit velocity in direction of $\dot{\rho} = 1$, this is later multiplied by $K_r(R_0-\rho) - K_V sgn(R_0-\rho)$ to make sure the radial separation is increasing or decreasing.

To check for stability of this control law, consider the following Lyapunov function

$$V(\rho, \phi) = \frac{1}{2}(\rho - R_0)^2 + \frac{1}{2}(\phi - \phi_0)^2 \tag{3.29}$$

The time derivative of this Lyapunov function gives us the following,

$$\dot{V}(\rho, \phi)) = (\rho - R_0)\dot{\rho} + (\phi - \phi_0)\dot{\phi}$$

where,

$$\begin{aligned}\dot{\rho} &= \gamma'(t) \cdot \begin{bmatrix}\cos(\phi)\\ \sin(\phi)\end{bmatrix} - \begin{bmatrix}\cos(\phi-\theta_F)\\ \sin(\phi-\theta_F)\end{bmatrix}(A(\alpha_F))_{2\times 2}U_F \\ \dot{\phi} &= \frac{1}{\rho}(\gamma'(t) \cdot \begin{bmatrix}-\sin(\phi)\\ \cos(\phi)\end{bmatrix} - \begin{bmatrix}-\sin(\phi-\theta_F)\\ \cos(\phi-\theta_F)]\end{bmatrix}(A(\alpha_F))_{2\times 2}U_F)\end{aligned} \tag{3.30}$$

Substituting the control law, U_F from 3.28 and using

$$\begin{aligned}&\dot{V}(\rho,\phi) = \\ &(\rho - R_0)(\gamma'(t)\begin{bmatrix}\cos(\phi)\\ \sin(\phi)\end{bmatrix} - (-K_V sgn(R_0-\rho) + K_r(R_0-\rho))) \\ &+ \frac{1}{\rho}(\phi-\phi_0)(\gamma'(t)\begin{bmatrix}-\sin(\phi)\\ \cos(\phi)\end{bmatrix} - (-K_V sgn(\phi_0-\phi) + K_\phi(\phi_0-\phi)))\end{aligned} \tag{3.31}$$

To further analyse this consider the following four cases,

1. $\rho > \mathbf{R_0}$ and $\phi > \phi_0$

   Using the above relation we can approximate

   $$\gamma'(t)\begin{bmatrix}\cos(\phi)\\ \sin(\phi)\end{bmatrix} < V_{max} \qquad \gamma'(t)\begin{bmatrix}-\sin(\phi)\\ \cos(\phi)\end{bmatrix} < V_{max} \tag{3.32}$$

   Using this inequality we can rewrite the time derivative of the Lyapunov function as follows

   $$\dot{V}(\rho,\phi) = -K_r(\rho-R_0)^2 + K_\phi(\phi-\phi_0)^2 - (K_V - V_{max})(\rho-R_0) - (K_V - V_{max})\frac{\phi-\phi_0}{\rho} \tag{3.33}$$

   Since, $K_V > V_{max}$ $\dot{V}(\rho,\phi) < 0$

2. $\rho < \mathbf{R_0}$ and $\phi > \phi_0$

   Using this relation, we can make the following approximations,

   $$\gamma'(t)\begin{bmatrix}\cos(\phi)\\ \sin(\phi)\end{bmatrix} \geq -V_{max} \qquad \gamma'(t)\begin{bmatrix}-\sin(\phi)\\ \cos(\phi)\end{bmatrix} \leq V_{max} \tag{3.34}$$

   Using these approximations we get the following value for $\dot{V}(\rho,\phi)$

   $$\dot{V}(\rho,\phi) = -K_r(\rho-R_0)^2 + K_\phi(\phi-\phi_0)^2 - (K_V - V_{max})(R_0-\rho) - (K_V - V_{max})\frac{\phi-\phi_0}{\rho} \tag{3.35}$$

3. $\rho < \mathbf{R_0}$ and $\phi < \phi_0$

   Again as before the following approximations can be made with respect to the assumptions 3.27.

$$\gamma'(t)\begin{bmatrix}\cos(\phi)\\ \sin(\phi)\end{bmatrix} \geq -V_{max} \qquad \gamma'(t)\begin{bmatrix}-\sin(\phi)\\ \cos(\phi)\end{bmatrix} \geq -V_{max} \tag{3.36}$$

   Using these assumptions, we get $\dot{V}$ is as follows,

$$\dot{V}(\rho,\phi) = -K_r(\rho - R_0)^2 + K_\phi(\phi - \phi_0)^2 - (K_V - V_{max})(R_0 - \rho) - (K_V - V_{max})\frac{\phi_0 - \phi}{\rho} \tag{3.37}$$

4. $\rho > \mathbf{R_0}$ and $\phi < \phi_0$

   Again as before the following approximations can be made with respect to the assumptions 3.27.

$$\gamma'(t)\begin{bmatrix}\cos(\phi)\\ \sin(\phi)\end{bmatrix} \leq V_{max} \qquad \gamma'(t)\begin{bmatrix}-\sin(\phi)\\ \cos(\phi)\end{bmatrix} \geq -V_{max} \tag{3.38}$$

   Using these we get the following,

$$\dot{V}(\rho,\phi) = -K_r(\rho - R_0)^2 + K_\phi(\phi - \phi_0)^2 - (K_V - V_{max})(\rho - R_0) - (K_V - V_{max})\frac{\phi_0 - \phi}{\rho} \tag{3.39}$$

Thus, in all the four cases, the Lyapunov function turns out to be less than zero for all $K_V > V_{max}$. In case of $\rho = R_0$ and $\phi = \phi_0$ with $\dot{V} = 0$ at $\rho = R_0$ and $\phi = \phi_0$. Hence, it is proved that this control law indeed tends to a radial separation of R_0 and angular orientation of ϕ_0. This completes the result.

It is currently very difficult to fabricate the Purcell's swimmer. But one of the possible limitations that we feel while fabricating the swimmer would to ensure a full rotational freedom to the links connecting the swimmer($\alpha_1, \alpha_2 \in [-\pi/2, \pi/2)$). Also, it is always advisable to use minimal amount of control energy as possible in order to make this formation problem more efficient. In the next section we exactly talk about all these things. We first talk about the optimal cost that we seek to minimize along with attaining the formation. We also talk about the possible issues that we need to first figure out before actually going on to solve this optimal control problem.

3.3 State Constrained Problem

The research to fabricate Purcell's swimmer is still at a primitive stage today with much of the research actually going about to designing actuators at this size. However, we do

believe that in a practical application there will be some constraint physical constraint on the swimmer which we hope to incorporate in this section.

One of the simplest possible constraint that one could think of would be a limit to the movement of the angles, α_1, α_2 in the swimmer. For example while designing a macro-prototype of the Purcell swimmer in our previous work [9] the side angles were constrained from $-\pi/2$ to $\pi/2$. In this section, we need to talk about leveraging our previous control algorithms in-order for them to satisfy this state inequality constraints.

One of the interesting part of the control algorithms that were explained earlier did not involve any specific assumptions about the Purcell swimmer in general. This speciality will be exploited for the state constrained problem by a simple linear transformation. Suppose in the formation control problems that were mentioned earlier, we wish to constrain the side angles within a range of β_1 to β_2. i.e $\alpha_1, \alpha_2 \in [\beta_1, \beta_2]$. To get around this, consider a simple transformation $T : [-\pi, \pi] \rightarrow [\beta_1, \beta_2]$ as follows,

$$T(\alpha') = \beta_1 * (\frac{\alpha' + \pi}{2\pi}) + \beta_2 \tag{3.40}$$

Using this simple transformation we can simply replace the angles α_1, α_2 by this simple transformation. As follows,

$$\begin{bmatrix} \dot{X} \\ \dot{Y} \\ \dot{\theta} \\ \dot{\alpha}'_1 \\ \dot{\alpha}'_2 \end{bmatrix} = \begin{bmatrix} \cos(\theta) & -\sin(\theta) & 0 \\ \sin(\theta) & \cos(\theta) & 0 \\ 0 & 0 & 1 \end{bmatrix} \begin{bmatrix} A(T(\alpha'_1), T(\alpha'_2)) \\ I \end{bmatrix} \begin{bmatrix} u_1 * (\beta_1/2\pi) \\ u_2 * (\beta_1/2\pi) \end{bmatrix} \tag{3.41}$$

Now, If we could simply call $A(T(\alpha'_1), T(\alpha'_2)) = A(\alpha')$ and $u'_1 = u_1 * (\beta_1/2\pi)$, $u'_2 = u_2 * (\beta_1/2\pi)$. We get a new set of equations that looks pretty similar to the old one as follows,

$$\begin{bmatrix} \dot{X} \\ \dot{Y} \\ \dot{\theta} \\ \dot{\alpha}'_1 \\ \dot{\alpha}'_2 \end{bmatrix} = \begin{bmatrix} \cos(\theta) & -\sin(\theta) & 0 \\ \sin(\theta) & \cos(\theta) & 0 \\ 0 & 0 & 1 \end{bmatrix} \begin{bmatrix} A'(\alpha') \\ I \end{bmatrix} \begin{bmatrix} u'_1 \\ u'_2 \end{bmatrix} \tag{3.42}$$

It can be noted here that the these equations look pretty similar to the ones that we started working with initially and the formation control algorithms that we described earlier can

be easily implemented keeping these in mind.

In the next section we summarise the results that we obtained after running our control algorithms as described in this chapter. We will also try to specify the potential pitfalls that were either observed or faced by us while going through the simulations.

Chapter 4

Results and Discussions

In this chapter we summarise the simulation results for the control algorithms that we proposed in the last chapter. In the next section we start talking about the circular formation problem that ran on our systems. In the section after this, we will be talking about the Leader-Follower kind of formation control results which will be later followed by the state constrained problem.

4.1 Circular formation

For the circular formation algorithm which was discussed in the earlier chapter we initialise the initial states of both the swimmers using a normal distribution and ran the simulations over at-least 10 runs before surmising our results here. In our circular formation problem we want to show that our control algorithm is able to attain a radial separation of $R_0 = 3.0$ which is shown in the figure 4.1. As shown in the figure 4.2 is the variation of control input with time. There are also variation of the side angles α_1, α_2 with time which is as shown in the figure 4.3, 4.4.

4.2 Leader Follower Formation

As shown in the figure 4.5 is the variation of the distance, ρ versus time steps where each time step is equivalent to 10^{-3} seconds. There are two important things to note about this, first, this control formulation does attain the desired radial separation of $R_0 = 6.0$ but it does so after a significant amount of semi-periodic kind of variation. We believe that two reasons could be attributed to this. The first one is the $sin(\Psi_1 - \Psi_2)$ term in the denominator of the control law. We know that, the zeros of this function is the $\alpha_1 + \alpha_2 = 0$ line which the function will invariably cross. Hence, we can see spikes that is due to these dip in the dynamical system manifold.

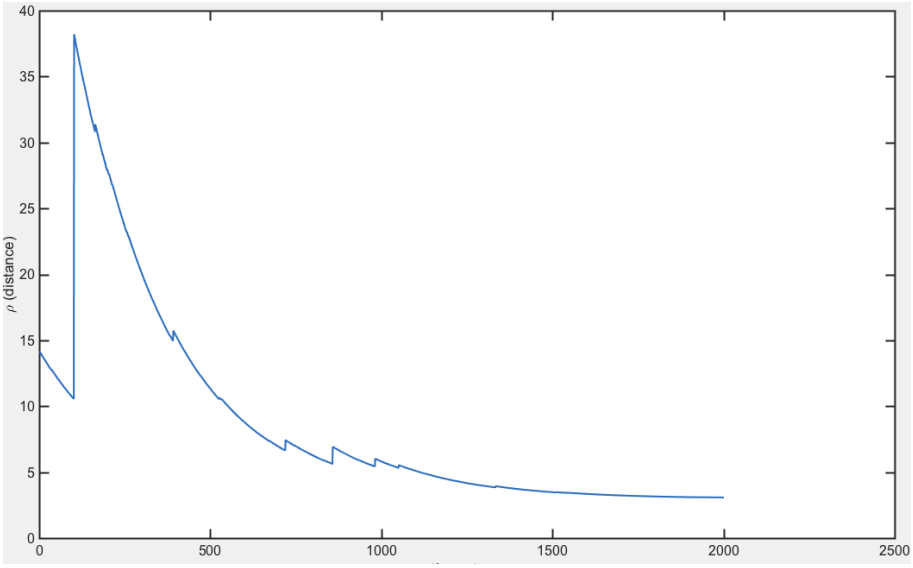

Figure 4.1: ρ vs time

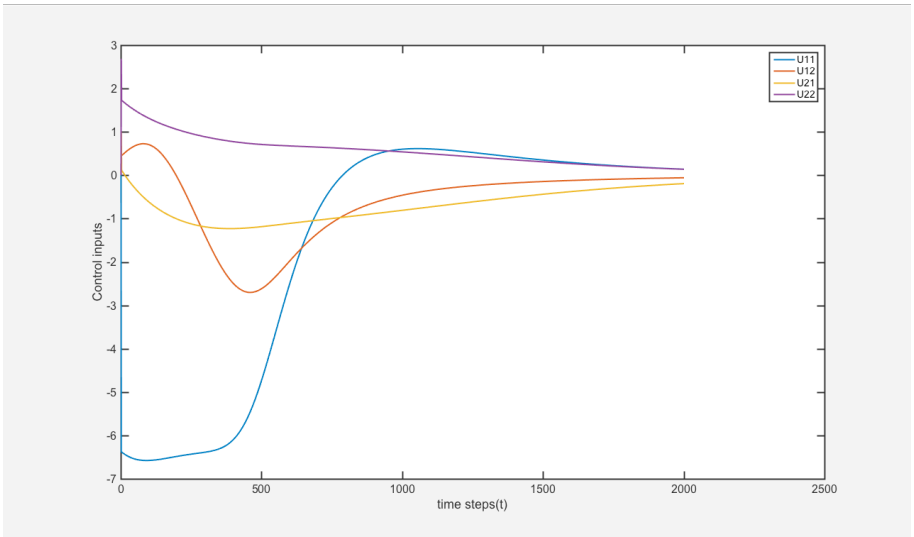

Figure 4.2: U_1, U_2 vs time

Since, $\gamma(t)$ is the unknown trajectory with a bounded velocity, we try our simulations for two different trajectories of the leader. The first of these is the sinusoidal motion in the state space as shown in the figure 4.7. As shown in the figure are the relevant ρ vs time and ϕ vs time steps as shown in the figure 4.6, 4.5. As can be seen in the ρ vs time plot, we can see that plot hovers around the desired separation of $R_0 = 6.0, \phi_0 = \pi/3$ but does-not attain it completely. This is because the $\gamma(t) = (t, \cos(10t))$ changes direction very frequently and hence it takes time to catch up with it.

In contrast to this, we also simulated our Leader-Follower formation on a simple straight line curve, $\gamma(t) = (t, t)$ as shown in the figure 4.10. Subsequent ρ, ϕ can be seen

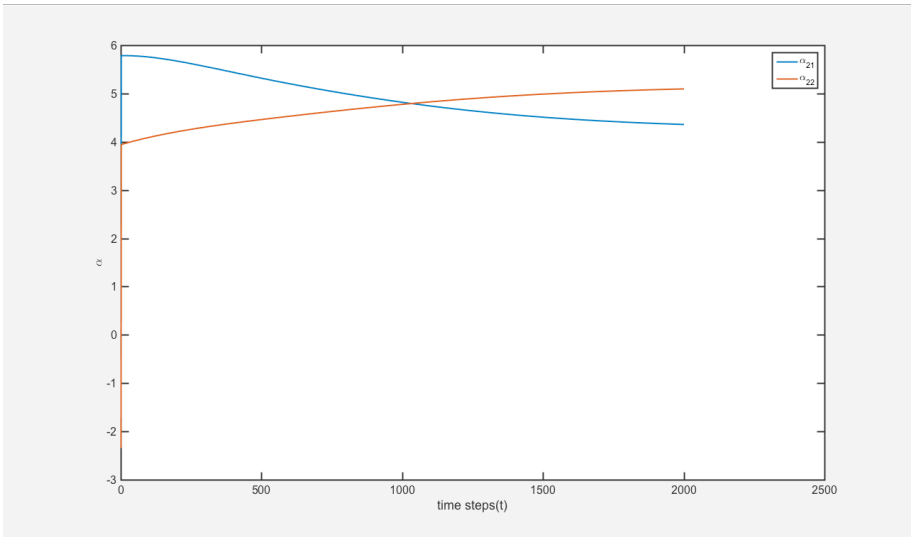

Figure 4.3: α_1 vs time

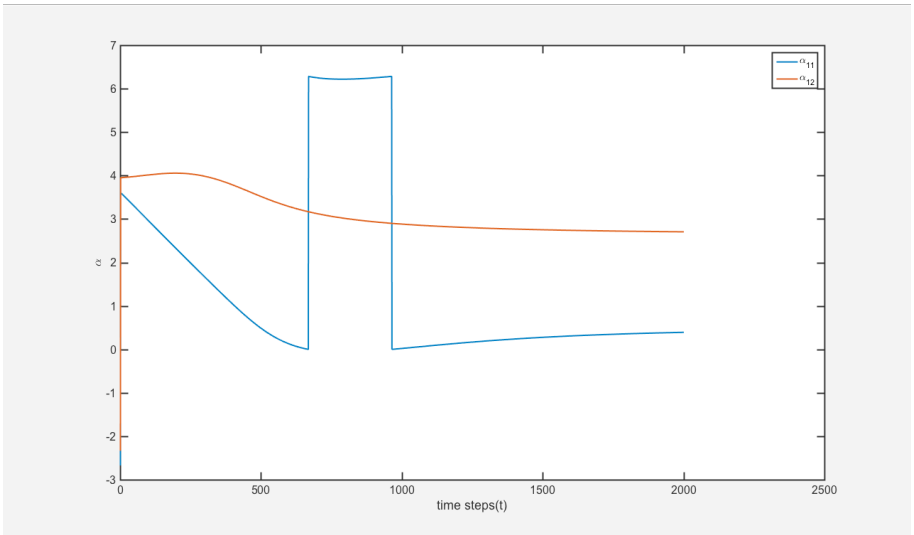

Figure 4.4: α_2 vs time

in figure 4.8, 4.9 respectively. Again since, the direction of $\gamma(t)$ we see that ρ plot doesnot take a lot of time to catch up with the desired separation.

It is important to note here that all the plots here were generated using random state initialisation. However, it is observed that the simulations does work better with normal state initialisation than a uniform initialisation which is something that needs to be investigated.

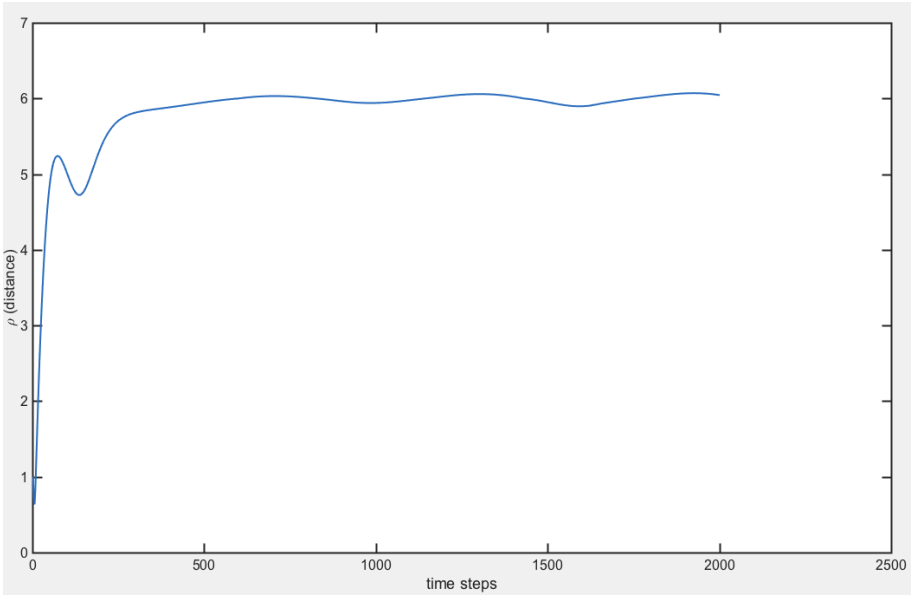

Figure 4.5: ρ vs time steps

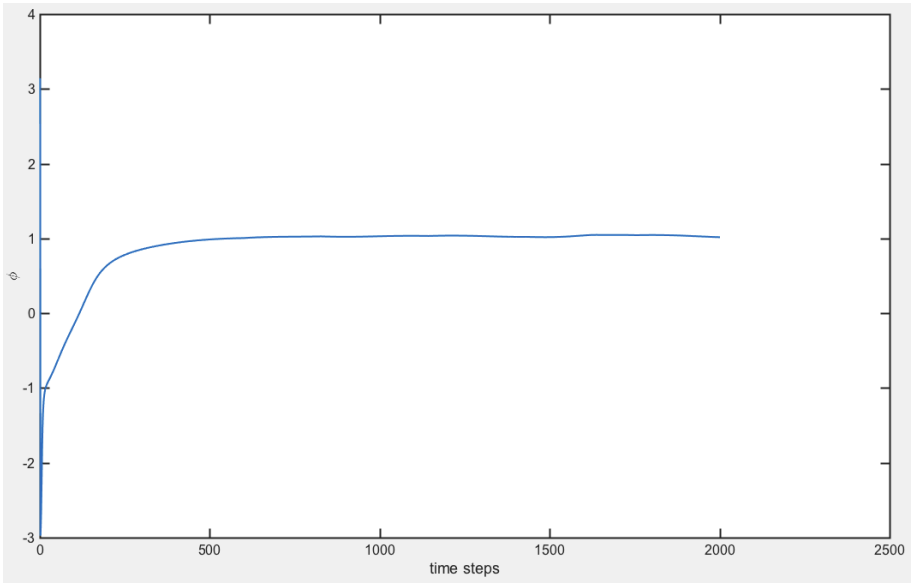

Figure 4.6: ϕ vs time steps

4.3 State Constrained Problem

In the constrained problem we wish to constrain our state space to a $\alpha_1, \alpha_2 \in [-pi/2, \pi/2]$ range. Hence the transformation that was proposed simply becomes, $T(\alpha')' = 2 * \alpha$. We tried our simulations with the circular formation with a radial separation of $R_0 = 3.0$ but with a state constraint as described above. The figure 4.11 is the plot of distance vs time steps which does reach the desired radial separation. However, the interesting plots are those of α_1 and α_2 with time as shown in the figures 4.12, 4.13 respectively. It can be

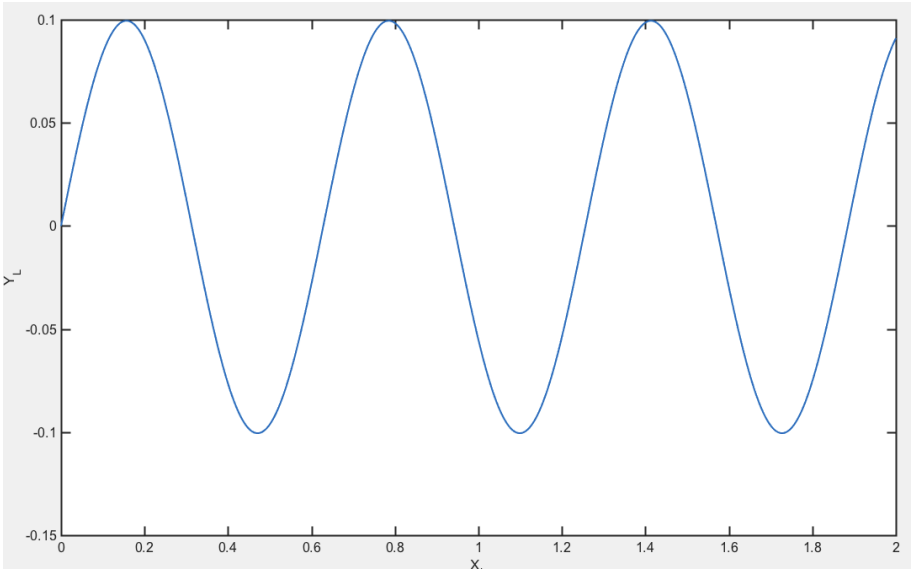

Figure 4.7: $\gamma(t) = (t, cos(10t))$

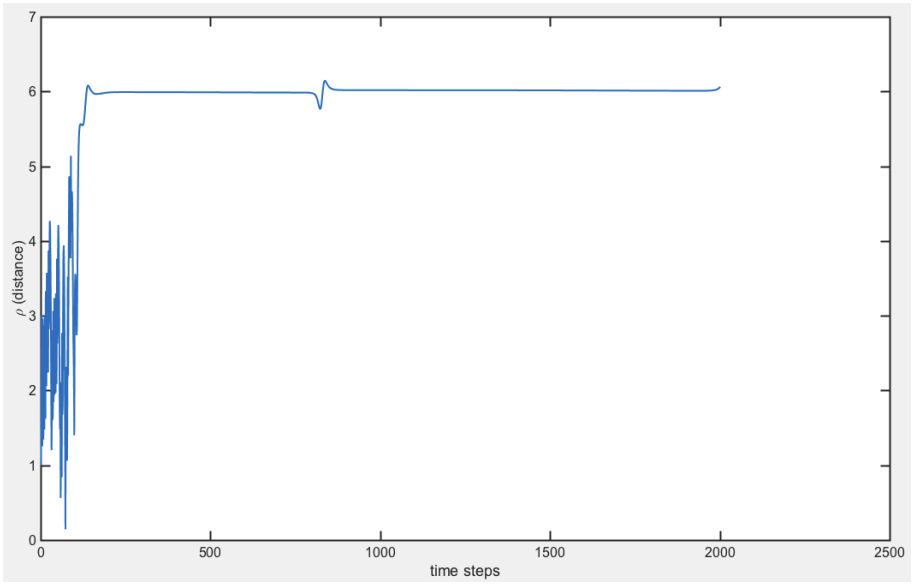

Figure 4.8: ρ vs time steps

seen clearly that these are constrained to required constraint.

A similar plot is shown for a leader-follower formation with state-constraints. We simulate the state-constraint for $\gamma(t) = (t, cos(10t))$. It can be seen easily from figures 4.14, 4.17 the plots of distance and ϕ with time and it does achieve the desired separation. It should be noted from, 4.15, 4.16 that the side angles does remain in the desired range but it does fluctuate a lot.

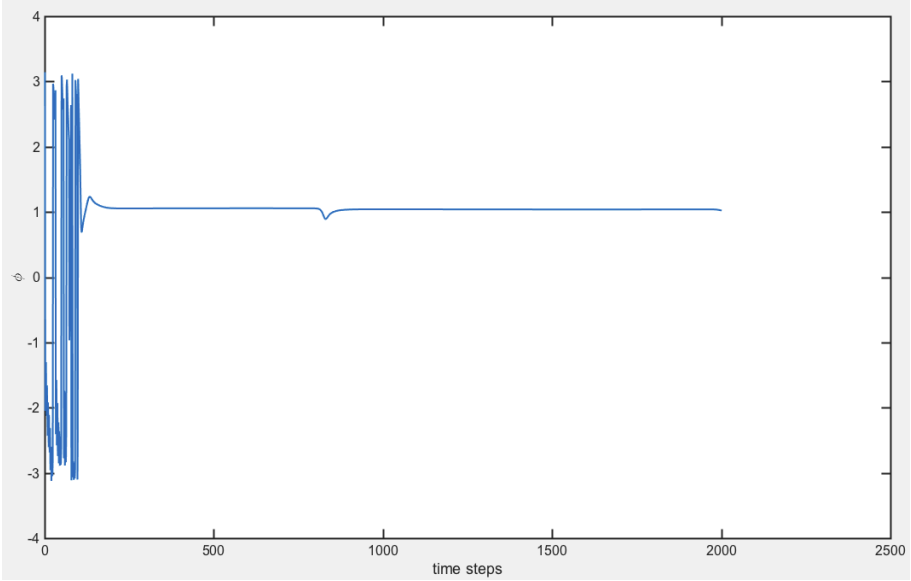

Figure 4.9: ϕ vs time steps

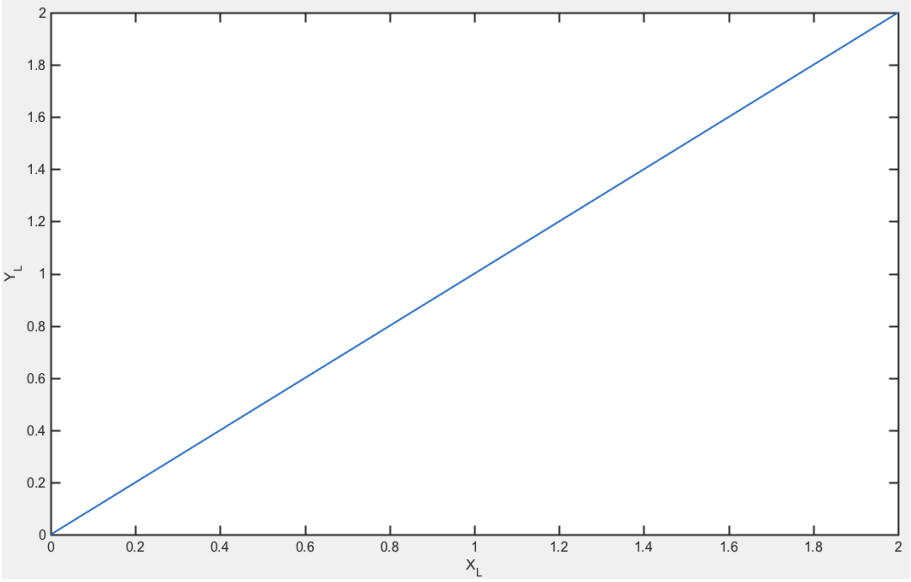

Figure 4.10: X_L vs Y_L

4.4 Conclusion

In this report we saw two types of formation which was achieved using a pair of Purcell's swimmers. In the first kind of formation, there was an attempt to achieve a circular kind of formation for a pair of Purcell's swimmers. We also show that there is a equilibrium point in the proposed control law which we characterize using symmetry operations on the Purcell's swimmers as mentioned in [6]. We further show the working of our control simulations by randomly initializing state variables.

In the next kind of formation, we talked about a leader swimmer which was moving with

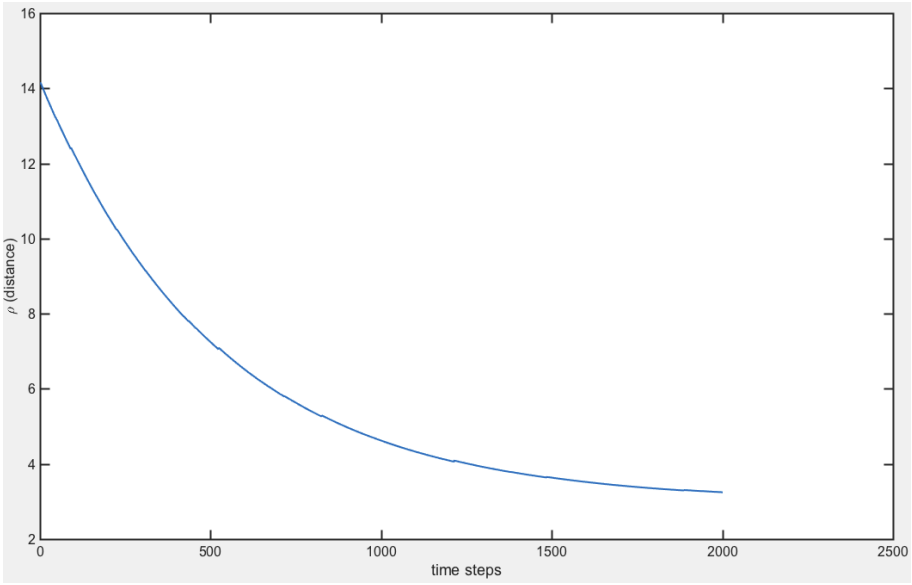

Figure 4.11: ρ vs time(State Constrained)

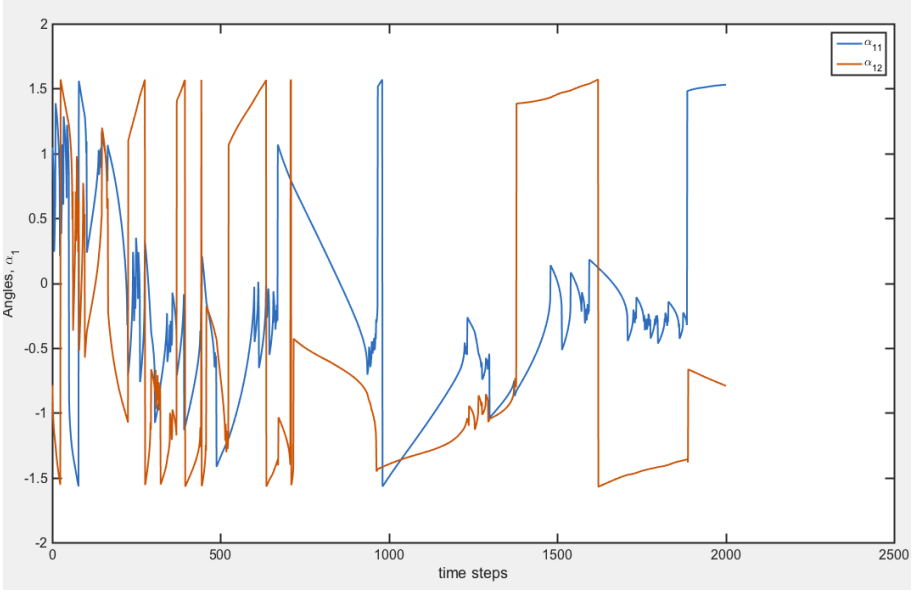

Figure 4.12: α_1 vs time(State Constrained)

a bounded velocity but unknown to the follower. Using a simple Lyapunov function we showed that the time derivative is negative for this swimmer but like before this also has equilibrium associated with it. We also show using simulations that the follower does manage to achieve the desired radial separation.

For future work, we wish to complete the proof of this formation problem to present a complete result on effectiveness of this control law. We wish to also expand this formation problem for a system of N-such swimmers to realise its potential application pitfalls.

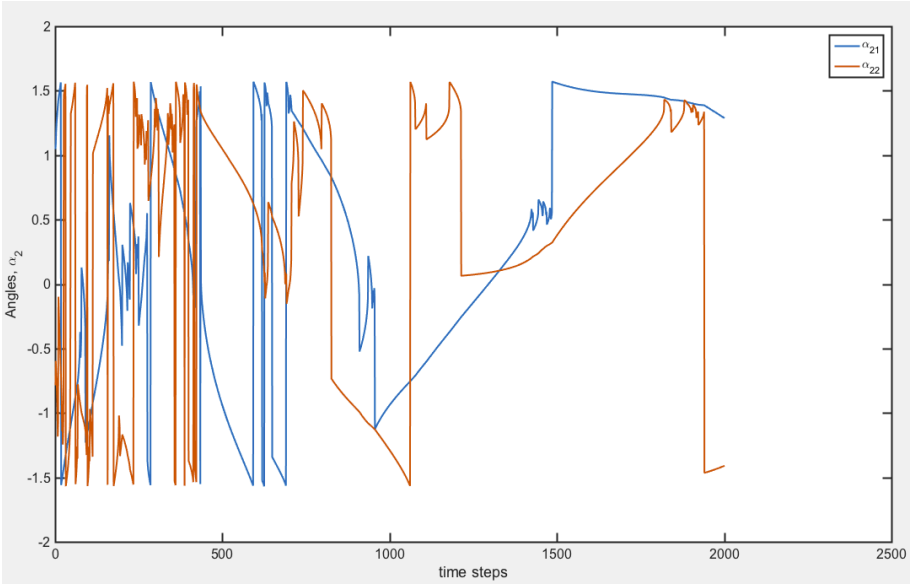

Figure 4.13: α_2 vs time(State Constrained)

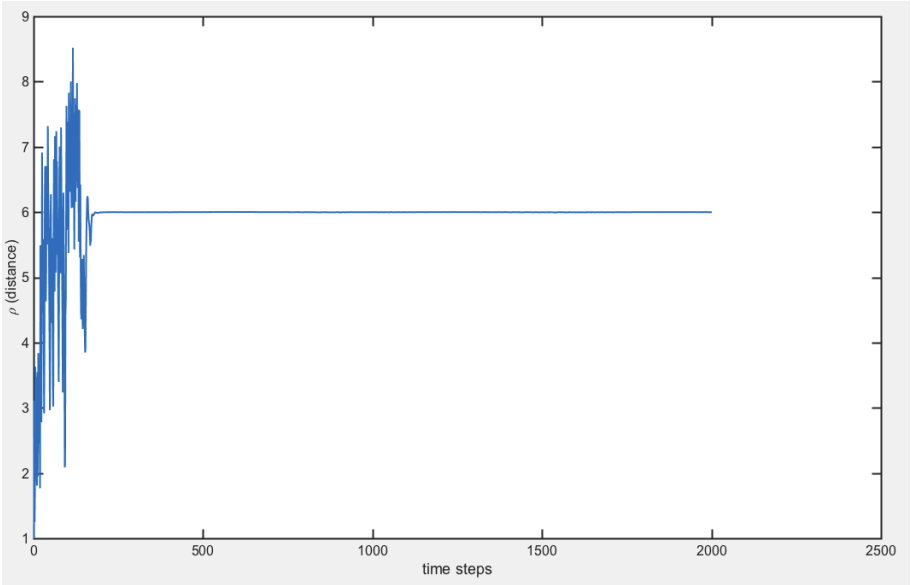

Figure 4.14: ρ vs time(State Constrained)

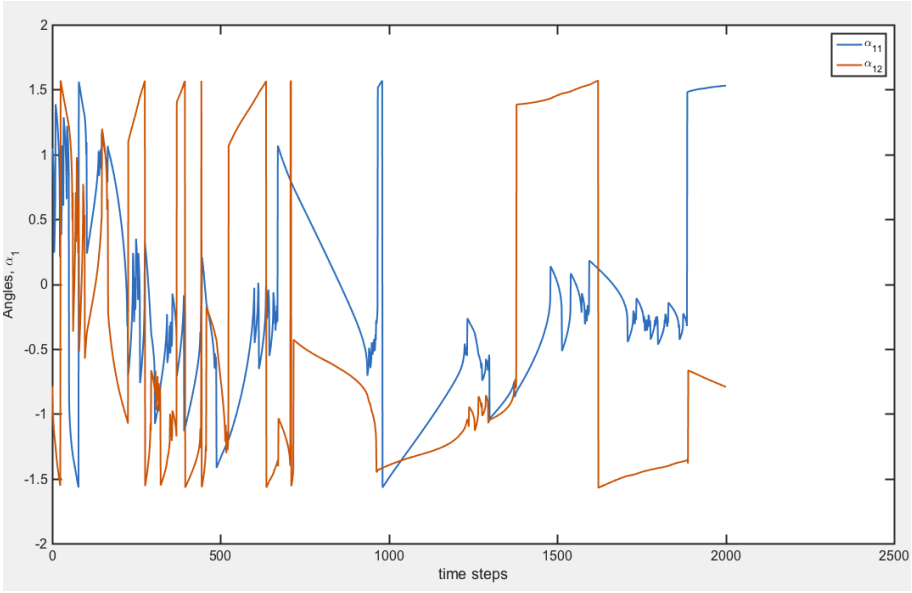

Figure 4.15: α_{F1} vs time(State Constrained)

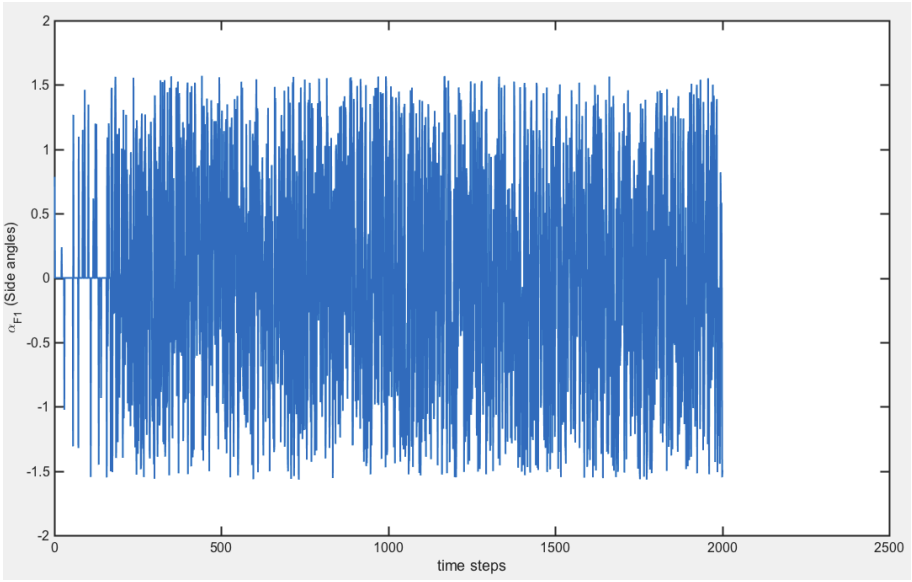

Figure 4.16: α_{F2} vs time(State Constrained)

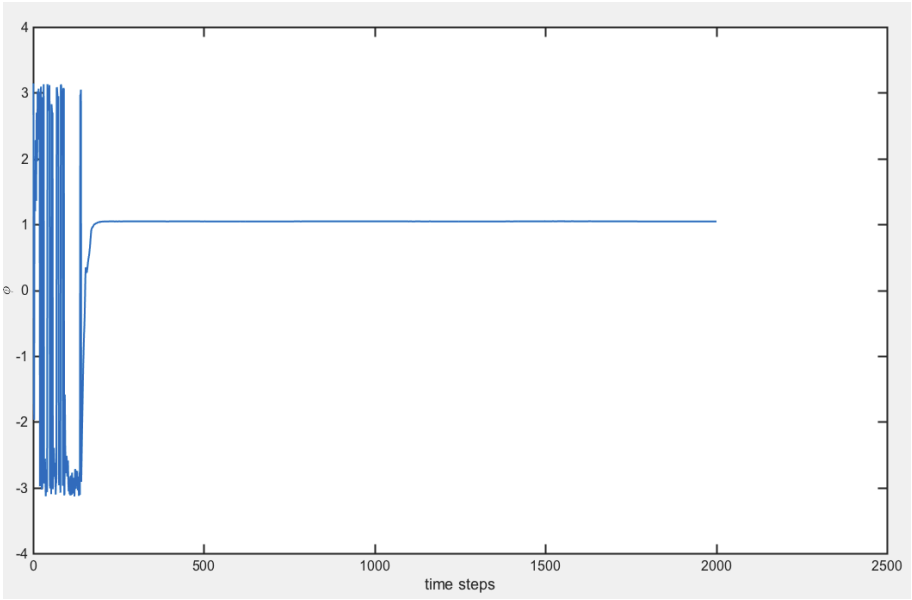

Figure 4.17: ϕ vs time(State Constrained)

References

[1] Balch, T. R., and Arkin, R. C., 1998, "Behavior-based formation control for multi-robot teams," *IEEE Trans. Robotics and Automation* **14**, 926–939.

[2] Chaillet, A., and Loría, A., 2008, "Uniform semiglobal practical asymptotic stability for non-autonomous cascaded systems and applications," *Automatica* **44**, 337–347.

[3] Cox, R. G., 1970, "The motion of long slender bodies in a viscous fluid part 1. general theory.." *Journal of Fluid mechanics* **44.04**, 791–810.

[4] Cui, R., Ge, S. S., How, B. V. E., and Choo, Y. S., 2009, "Leader-follower formation control of underactuated auvs with leader position measurement," in *2009 IEEE International Conference on Robotics and Automation, ICRA 2009, Kobe, Japan, May 12-17, 2009*, pp. 979–984.

[5] Ge, S. S., and Fua, C., 2005, "Queues and artificial potential trenches for multirobot formations," *IEEE Trans. Robotics* **21**, 646–656.

[6] Gutman, E., and Or, Y., 2016, "Symmetries and gaits for purcell's three-link microswimmer model," *IEEE Trans. Robotics* **32**, 53–69.

[7] Hatton, R. L., and Choset, H., 2013, "Geometric swimming at low and high reynolds numbers," *IEEE Trans. Robotics* **29**, 615–624.

[8] Justh, E. W., and Krishnaprasad, P. S., 2004, "Equilibria and steering laws for planar formations," *Systems & Control Letters* **52**, 25–38.

[9] Kadam, S., Joshi, K., Gupta, N., Katdare, P., and Banavar, R. N., 2017, "Trajectory tracking using motion primitives for the purcell's swimmer," in *2017 IEEE/RSJ International Conference on Intelligent Robots and Systems, IROS 2017, Vancouver, BC, Canada, September 24-28, 2017*, pp. 3246–3251.

[10] Khalil, H., 2002, *Nonlinear Systems*, Pearson Education (Prentice Hall). ISBN 9780130673893

[11] Lewis, M. A., and Tan, K., 1997, "High precision formation control of mobile robots using virtual structures," *Auton. Robots* **4**, 387–403.

[12] Purcell, E., 1977, "Life at low reynolds number," *American Journal of Physics* **311**

Acknowledgements

I would like to thank Prof. Ravi Banavar and Prof. Salil Kulkarni for their continued guidance and support all through the duration of the Thesis. I would also like to thank Sudin Kadam for his constructive criticism throughout the duration of this thesis.

Pulkit Katdare
IIT Bombay
5 September 2023